Published October 6, 2009

T-bet–dependent $S1P_5$ expression in NK cells promotes egress from lymph nodes and bone marrow

Craig N. Jenne,[1,2] Anselm Enders,[3] Richard Rivera,[4] Susan R. Watson,[1] Alexander J. Bankovich,[1,2] Joao P. Pereira,[1,2] Ying Xu,[1,2] Carla M. Roots,[3] Joshua N. Beilke,[1] Arnob Banerjee,[5] Steven L. Reiner,[5] Sara A. Miller,[6] Amy S. Weinmann,[6] Chris C. Goodnow,[3] Lewis L. Lanier,[1] Jason G. Cyster,[1,2] and Jerold Chun[4]

[1]Department of Microbiology and Immunology and [2]Howard Hughes Medical Institute, University of California, San Francisco, San Francisco, CA 94143
[3]Ramaciotti Immunization Genomics Laboratory, John Curtin School of Medical Research, Australian National University, Canberra ACT 0200, Australia
[4]Department of Molecular Biology, Helen L. Dorris Child and Adolescent Neuropsychiatric Disorder Institute, The Scripps Research Institute, La Jolla, CA 92037
[5]Abramson Family Cancer Research Institute, University of Pennsylvania, Philadelphia, PA 19104
[6]Department of Immunology, University of Washington, Seattle, WA 98195

During a screen for ethylnitrosourea-induced mutations in mice affecting blood natural killer (NK) cells, we identified a strain, designated Duane, in which NK cells were reduced in blood and spleen but increased in lymph nodes (LNs) and bone marrow (BM). The accumulation of NK cells in LNs reflected a decreased ability to exit into lymph. This strain carries a point mutation within *Tbx21* (T-bet), which generates a defective protein. Duane NK cells have a 30-fold deficiency in sphingosine-1-phosphate receptor 5 ($S1P_5$) transcript levels, and $S1P_5$-deficient mice exhibit an egress defect similar to Duane. Chromatin immunoprecipitation confirms binding of T-bet to the *S1pr5* locus. S1P-deficient mice exhibit a more severe NK cell egress block, and the FTY720-sensitive $S1P_1$ also plays a role in NK cell egress from LNs. $S1P_5$ is not inhibited by CD69, a property that may facilitate trafficking of activated NK cells to effector sites. Finally, the accumulation of NK cells within BM of S1P-deficient mice was associated with reduced numbers in BM sinusoids, suggesting a role for S1P in BM egress. In summary, these findings identify $S1P_5$ as a T-bet–induced gene that is required for NK cell egress from LNs and BM.

CORRESPONDENCE
Jason G. Cyster:
Jason.Cyster@ucsf.edu
OR
Lewis L. Lanier:
lewis.lanier@ucsf.edu
OR
Jerold Chun:
jchun@scripps.edu

Abbreviations used: ChIP, chromatin immunoprecipitation; ENU, ethylnitrosourea; HA, hemagglutinin; iNKT, invariant NKT; LCMV, lymphocytic choriomeningitis; S1P, sphingosine-1-phosphate; $S1P_1$, S1P receptor 1; SNP, single nucleotide polymorphism.

After development in the BM, NK cells are released into circulation and are found in large numbers in the spleen and liver. Recent studies have also highlighted the presence of NK cells within LNs (Martín-Fontecha et al., 2004; Chen et al., 2005; Bajénoff et al., 2006; Garrod et al., 2007; Walzer et al., 2007a), accounting for ∼0.5% of cells in mouse LNs and ∼5% in human LNs (Grégoire et al., 2007). After immunization or infection, NK cell numbers can increase rapidly within draining LNs (Martín-Fontecha et al., 2004; Lucas et al., 2007; Gustafsson et al., 2008; Watt et al., 2008). Accumulating evidence suggests that NK cells help shape the adaptive immune response emerging within a responding lymphoid tissue (Martín-Fontecha et al., 2004; Bajénoff et al., 2006; Kassim et al., 2009). LNs and spleen are also likely to be early sites of NK encounter with inflammatory stimuli presented, for example, by dendritic cells. A recent study has provided evidence that NK cells can be primed in draining LNs before returning to the circulation with enhanced effector function (Lucas et al., 2007). Moreover, several recent studies have identified requirements for NK cell entry into LNs (Martín-Fontecha et al., 2004; Chen et al., 2005;

A. Enders and R. Rivera contributed equally to this paper.

The Rockefeller University Press $30.00
J. Exp. Med. Vol. 206 No. 11 2469-2481
www.jem.org/cgi/doi/10.1084/jem.20090525

Supplemental Material can be found at:
http://jem.rupress.org/content/suppl/2009/10/05/jem.20090525.DC1.html

Published October 6, 2009

Bajénoff et al., 2006; Lucas et al., 2007); however, less is understood about how they return to circulation.

T cell egress from thymus, and T and B cell egress from peripheral lymphoid organs depends on sphingosine-1-phosphate (S1P) and S1P receptor 1 ($S1P_1$; Allende et al., 2004; Matloubian et al., 2004; Pappu et al., 2007). In contrast, $S1P_1$ and S1P deficiency have not been found to block B cell egress from BM (Matloubian et al., 2004; Pappu et al., 2007). FTY720, a small molecule that can down-modulate $S1P_1$, is also effective in preventing T and B cell egress from thymus and LNs (Mandala et al., 2002; Gräler and Goetzl, 2004; Matloubian et al., 2004). However, FTY720 treatment does not deplete NK cells from circulation in mice or humans (Vaessen et al., 2006; Walzer et al., 2007b). NK cells selectively express $S1P_5$, and in mice deficient in this receptor, NK cell distribution was altered, with reduced NK cell numbers in blood and spleen and increased numbers in LNs and BM (Walzer et al., 2007b). This work established a role for $S1P_5$ in NK cell recirculation; however, $S1P_5$'s role in egress was not defined.

T-bet is a T-box–containing transcription factor that is required for Th1 cell development and also functions in the generation of effector $CD8^+$ T cells and in B cells for switching to IgG2a (Szabo et al., 2000; Peng et al., 2002; Lugo-Villarino et al., 2003; Xu and Zhang, 2005; Joshi et al., 2007; Intlekofer et al., 2008). T-bet is also required for the final maturation of NK cells and for the development of invariant NKT (iNKT cells; Townsend et al., 2004). T-bet has been shown to mediate direct effects on various promoters, to bind and modify the effects of other transcription factors, and to facilitate chromatin remodeling through the regulation of histone methyltransferase activity (Hwang et al., 2005; Mehta et al., 2005; Beima et al., 2006; Chen et al., 2006; Djuretic et al., 2007; Lewis et al., 2007). The key genes regulated by T-bet in NK cell development and maturation are not well defined.

In an effort to identify genes involved in NK cell development or trafficking, we screened mice carrying ethylnitrosourea (ENU)-induced mutations for altered blood NK cell numbers or surface phenotypes. Our characterization of a strain with low circulating NK cells led us to identify a role for T-bet in promoting $S1P_5$ expression in several cell types and to establish a role for $S1P_5$ in NK cell egress from LNs and BM.

RESULTS

Characterization of the ENU strain Duane

Screening peripheral blood for lymphocyte phenotypes resulting from ENU-induced mutations identified a strain, Duane, with a low percentage of NK cells in the blood, spleen, and liver, but a significantly elevated frequency of NK cells in peripheral LNs and BM (Fig. 1 A; and Fig. S1, A and B). The blood samples were also screened for CD69, with the intent of detecting mutations that altered the ability of CD69 to regulate lymphocyte egress (Shiow et al., 2006). An increased fraction of Duane NK cells was found to express CD69 (Fig. 1 B). Through further flow cytometric analysis of various developmental markers, Duane NK cells were found to have the $CD27^{hi}KLRG1^{lo}$ phenotype typical of immature NK cells (Fig. 1 B). Duane had a near complete absence of mature iNKT cells (Fig. S1 A).

To determine if the NK cell accumulation in peripheral LNs was cell intrinsic, mixed BM chimeras were generated. In these mice, a lower percentage of Duane NK cells was observed in blood and spleen as compared with wild-type NK cells, whereas there was a relative accumulation of Duane NK cells in peripheral LNs (Fig. 2 A). The distribution of Duane and wild-type B cells was examined as a control and was equivalent in all sites (Fig. 2 A). Analysis of the lymph from these mice revealed an underrepresentation of Duane NK cells, suggesting that the LN accumulation was caused by a failure of these cells to egress (Fig. 2 A). When mixed BM chimeras were treated with α4 integrin, αL integrin, and L-selectin blocking antibodies to prevent NK cell and lymphocyte entry into LNs (von Andrian and Mempel, 2003; Bajénoff et al., 2006; Pham et al., 2008), and the extent of decay in LN cell numbers was measured after 40 h, an increase in the percentage of Duane NK cells was observed (Fig. 2 A). This finding was consistent with a reduction in the ability of Duane NK cells to exit LNs. In another test of trafficking behavior, wild-type and Duane splenocytes were each transferred into wild-type B6 recipients, and 24 h later the ratio of donor NK cells in the LN versus spleen was calculated. A greater fraction of Duane NK cells was found in the LNs as compared with wild-type NK cells, consistent with a defect in Duane NK cell egress from peripheral LNs (Fig. 2 B).

Identification of the Duane mutation

Mapping the causative genetic lesion in Duane was achieved by crossing an affected Duane mouse onto a wild-type C57BL/10 mouse, followed by intercrossing these F1 offspring and screening for the Duane phenotype. The seven most clearly affected and eight clearly unaffected mice were selected for the initial genome scan. Mapping was performed as previously described (Nelms and Goodnow, 2001) by using a panel of 80 Amplifluor assays that can distinguish single nucleotide polymorphisms (SNPs) between C57BL/6 and C57BL/10. The only clear linkage was for markers on the distal part of chromosome 11, and all mice were typed for these markers individually (Fig. S2 A). Because of a lack of markers that are capable of distinguishing between C57BL/6 and C57BL/10 in the region distal to 79 Mbp on chromosome 11, we set up a second round of mapping by crossing an affected Duane mouse with a wild-type CBA/J mouse, followed by backcrossing to another affected Duane mouse. The resulting N2 mice were tested for the Duane phenotype and genotyped for SNPs distinguishing CBA/J and C57BL/6 genomes on distal chromosome 11. This strategy confirmed linkage to a region between 89.3 and 116.1 Mbp on chromosome 11 (Fig. S2 B).

A search of the Mouse Genome Database (available at http://www.informatics.jax.org/; Bult et al., 2008) for genes in this interval identified *Tbx21* as a likely candidate. Sequencing the genomic DNA corresponding to the gene

Published October 6, 2009

encoding T-bet, *Tbx21*, identified a point mutation resulting in the replacement of a single nucleotide in the second intron (Fig. S2, C and D). This mutation disrupts an intronic splice acceptor site, thereby preventing the normal splicing of the T-bet mRNA (Fig. S2, E and F). PCR amplification and sequencing of T-bet mRNA isolated from Duane splenocytes revealed the use of a cryptic intronic splice acceptor site located 24 nucleotides into exon 3 (Fig. S2, F and G). This results in a predicted, in-frame, eight–amino acid deletion in the deduced protein sequence of Duane T-bet (Fig. S2 G). Comparison of the predicted protein structure of Duane T-bet to the known structure of the T-box domain of *Xenopus laevis* T protein and the predicted structures of other mammalian T-box proteins indicates that this deletion corresponds to a region adjacent to and including one of the residues involved in known protein–protein interactions (Fig. S2 H).

Expression of T-bet in Duane

PCR analysis of T-bet mRNA levels using primers spanning exons 1 and 2 indicated little difference between Duane and wild-type NK cells (Fig. S2 I). To assay T-bet protein levels, splenocytes were cultured for 48 h in conditions conducive to polyclonal T cell activation. Although both Duane and wild-type splenocytes activated to the same degree (Fig. S2 J), the amount of T-bet protein in Duane cell lysates were three- to fourfold lower than those of wild-type mice (Fig. S2 K). Interestingly, although some T-bet protein was detected in Duane, the NK phenotype of this strain was indistinguishable from that of T-bet–null mice (Fig. 1 B), and both strains exhibit a severe deficiency in iNKT cells (Fig. S1; Townsend et al., 2004).

T-bet function in Duane

To determine if the Duane mutation affected the function of T-bet, cells were transfected with an empty vector or a vector encoding wild-type or Duane T-bet, and the transcription of various gene targets was assayed. Overexpression of wild-type T-bet resulted in greater than fivefold induction in the transcription of IFN-γ, CCL3, and CXCR3 (Fig. S3 A). In contrast, overexpression of Duane T-bet did not result in the increased transcription of any of these known T-bet target genes, suggesting that the Duane mutation has rendered

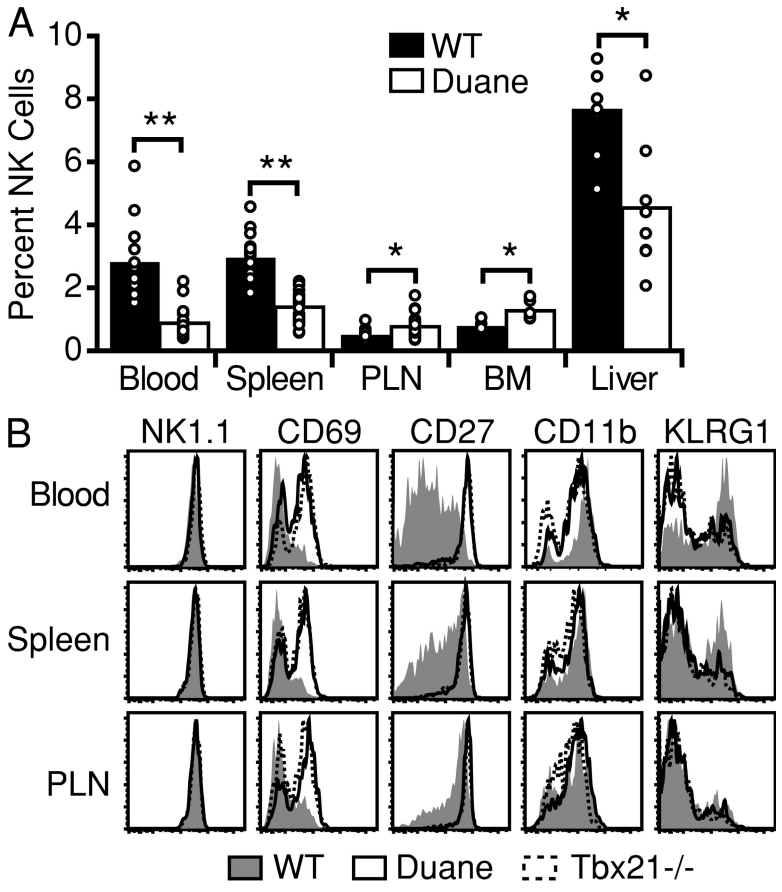

Figure 1. Identification of the ENU mutant Duane. (A) NK cell frequencies within the indicated tissues of Duane and wild-type B6 mice. Bars represent mean values, and circles represent individual animals. Data are representative of at least two Duane and two wild-type mice in each of three independent experiments. (B) Representative flow cytometric analysis of NK cells from Duane, *Tbx21*$^{-/-}$, and wild-type B6 mice for cell-surface markers. Plots are representative of at least three independent experiments, each analyzing at least two Duane and two wild-type mice. PLN, peripheral LN. *, $P < 0.005$; **, $P < 0.0001$.

Published October 6, 2009

T-bet nonfunctional. Additionally, cotransfection of cells with a vector containing Duane T-bet and a luciferase reporter coupled to the mouse IFN-γ promoter region failed to result in an increase in luciferase activity, whereas transfection of a wild-type T-bet vector together with the reporter construct resulted in robust luciferase activity (Fig. S3 B).

To further test if any T-bet function remained in Duane, we analyzed both T and B cell differentiation in assays previously demonstrated to be T-bet dependent. Mixed cultures of wild-type and Duane T cells under Th1-inducing conditions failed to result in the expression of IFN-γ within the Duane cells despite robust expression in the co-cultured wild-type cells (Fig. S3 C). This result was similar to that observed in a wild-type and T-bet–deficient cell co-culture (Fig. S3 C). Likewise, co-culture of wild-type and Duane B cells under IgG2a-inducing conditions resulted in expression of IgG2a by the CD45.1$^+$ wild-type cells but not the Duane B cells (Fig. S3 D). From these assays, the Duane mutation appears to result in a functionally null T-bet phenotype.

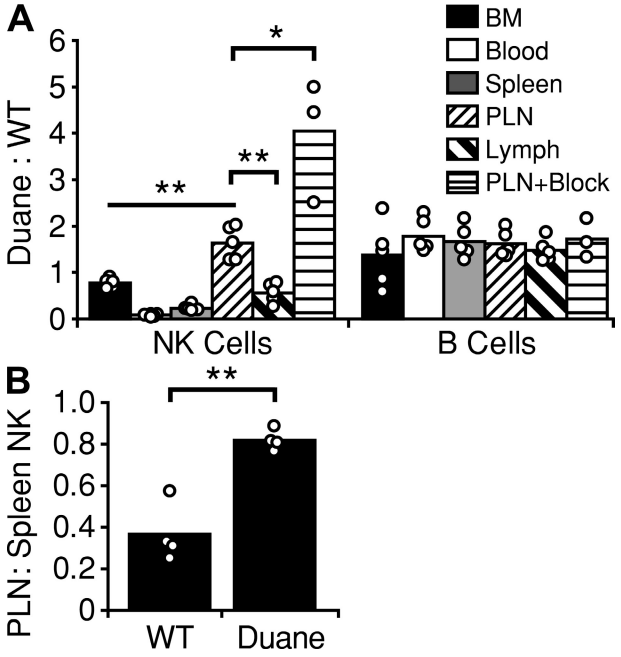

Figure 2. Peripheral lymph node NK cell accumulation in Duane results from a cell-intrinsic egress defect. (A) Analysis of wild-type mice reconstituted with a mix of wild-type and Duane BM. Some mice (PLN+Block) received integrin and selectin blocking antibodies 40 h before analysis. Values are reported as a ratio of Duane (CD45.2) to wild-type (CD45.1) cells. At least two untreated and two treated chimeras were analyzed in each of two independent experiments. (B) Analysis of wild-type B6 mice 24 h after adoptive transfer of either Duane or wild-type splenocytes. Values are reported as a ratio of transferred NK cells recovered from the spleen (as a percentage of transferred B cells) to transferred NK cells in the peripheral LNs (as a percentage of transferred B cells). Data were obtained from two independent experiments, each composed of two recipients receiving Duane splenocytes and two recipients receiving wild-type splenocytes. Bars represent mean values, and circles represent individual animals. PLN, peripheral lymph node. *, $P < 0.005$; **, $P < 0.001$.

T-bet regulation of $S1P_5$

In an effort to understand the mechanism behind the NK cell accumulation in Duane LNs, we analyzed the expression of S1P receptors in NK cells. NK cells were notable in their abundant expression of $S1P_5$ (Fig. 3 A; Barrett et al., 2007), as reported previously (Walzer et al., 2007b), but they also expressed $S1P_1$ (Fig. 3 A). A comparison of Duane and wild-type NK cells revealed markedly reduced amounts of $S1P_5$ in Duane NK cells but comparable amounts of $S1P_1$ between the two groups (Fig. 3 B).

To explore the possibility that T-bet was a regulator of $S1P_5$ expression, T-bet was overexpressed in WEHI-231 cells and in primary CD4$^+$ and CD8$^+$ T cells (Fig. 3 C). In each case, transduction of cells with a vector containing T-bet was sufficient to induce $S1P_5$ expression. Although only low levels of $S1P_5$ expression were achieved in WEHI-231 cells, the magnitude of this induction was similar to that of the known T-bet target IFN-γ (Fig. 3 C). To determine if T-bet acted directly on the *S1pr5* locus, binding to conserved 5′ and 3′ regions of the gene was examined. T-bet chromatin immunoprecipitation (ChIP) using lysates from cell types known to abundantly express T-bet (Th1 cells and effector CD8$^+$ T cells) demonstrated an interaction of T-bet with a 3′ site (Fig. 3 D).

We addressed whether other cell types that express T-bet show $S1P_5$ expression. iNKT cells were found to have high $S1P_5$ expression (Fig. 3 E). The failure of iNKT cells to develop in the absence of T-bet prevented us from further testing the connection between T-bet and $S1P_5$ expression in these cells. Sorted CD44^{hi} CD4$^+$ and CD8$^+$ T cells, representing memory and/or effector T cell populations, freshly isolated from adult mice showed low but measurable $S1P_5$ expression as well as T-bet, and the $S1P_5$ transcripts were reduced by >50-fold in cells sorted from T-bet–deficient mice (Fig. 3 E). Finally, when CD8$^+$ T cells were stimulated with antigen under culture conditions that promote development of T-bet–expressing effector cells (Intlekofer et al., 2008), there was marked up-regulation of $S1P_5$ and this was dependent on intrinsic T-bet expression (Fig. 3 F). Thus, T-bet promotes the expression of the egress receptor $S1P_5$ in NK cells and CD8$^+$ effector T cells, and likely also in iNKT cells.

S1P and S1P receptor requirement for NK cell egress from LNs

In initial experiments to elucidate the contribution of S1P receptors to NK cell egress from secondary lymphoid tissues, mice were treated for 20 h with FTY720, and analyzed for NK cell and T and B cell numbers in lymph. As previously reported, FTY720 treatment resulted in a near complete absence of T or B cells from the lymph (Fig. 4 A; Mandala et al., 2002; Matloubian et al., 2004). NK cells, however, were present in the lymph but were reduced in number as compared with saline-treated animals (Fig. 4 A). When mice were treated with integrin and selectin blocking antibodies to prevent NK cell and lymphocyte entry into lymph nodes, additional treatment with FTY720 prevented the egress-mediated

Published October 6, 2009

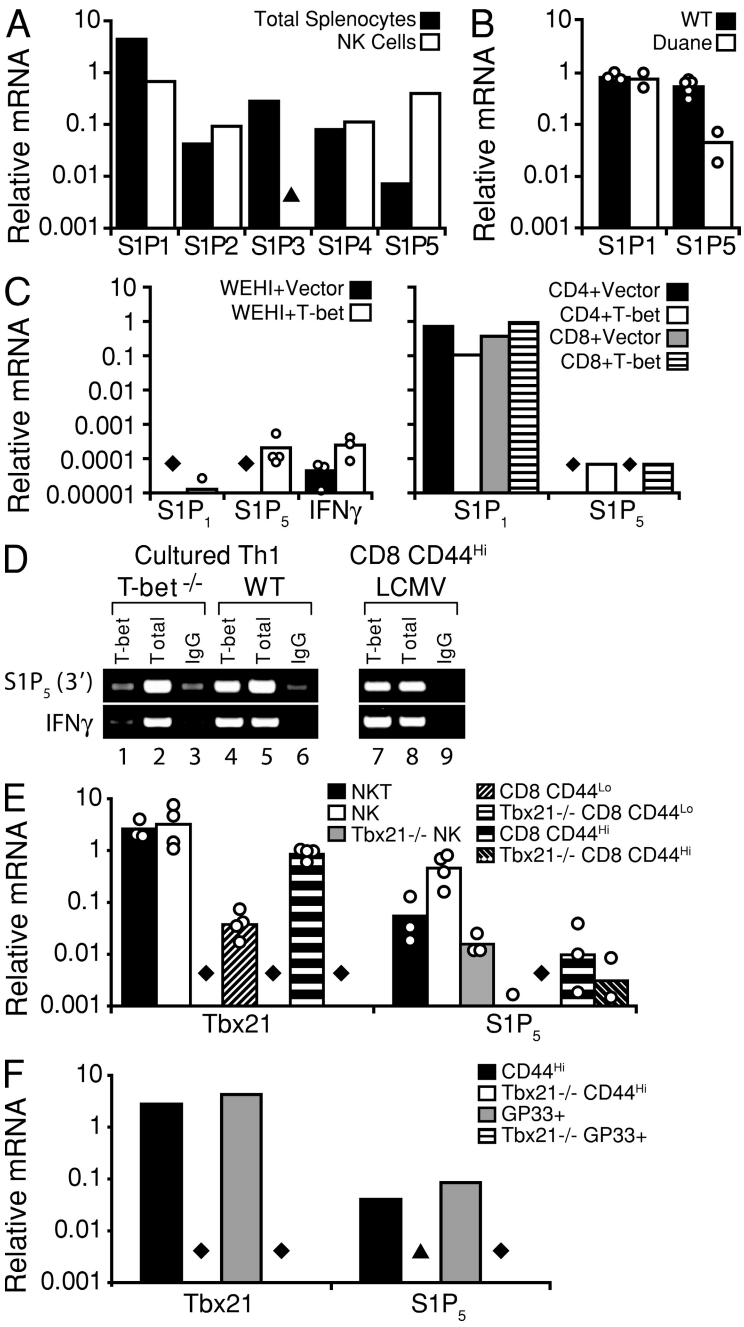

Figure 3. Reduced $S1P_5$ but not $S1P_1$ expression in Duane cells and T-bet–mediated induction of $S1P_5$ expression. (A–C) Quantitative PCR analysis of S1PR or IFN-γ transcript expression in (A) total splenocytes and sorted splenic NK cells from a wild-type mouse, (B) wild-type and Duane splenic NK cells (bars represent mean values, and circles represent sorted NK samples from individual animals), and (C) either vector- or T-bet–transduced WEHI-231 cells (left; bars represent mean values, and circles represent individual transductions) or primary T cells (right; bars represent individual transductions). (D) T-bet associates with the region 3′ of the *S1pr5* gene. Primary $CD4^+$ T cells were isolated from either *Tbx21*$^{-/-}$ (lanes 1–3) or wild-type (lanes 4–6) mice, and were polarized in Th1 conditions for 6 d (results are representative of two independent experiments, each using cells pooled from two individual animals). $CD8^+$ T cells were isolated from mice infected with LCMV (lanes 7–9; results are representative of two independent immunoprecipitations using cells pooled from three individual animals). A standard ChIP analysis was then performed with a T-bet–specific antibody (lanes 1, 4, and 7) or an IgG control (lanes 3, 6, and 9). A standardized aliquot of the input chromatin was also examined as a control. Gene-specific primers were used to amplify the ChIP samples, as indicated to the left of the gel images. (E and F) Quantitative PCR analysis of T-bet or $S1P_5$ transcript expression in (E) various lymphocyte subsets sorted from naive wild-type or T-bet–deficient mice (bars represent mean values, and circles represent sorted cell samples from individual animals; data were obtained from three independent experiments), and (F) in vitro–generated, sorted, polyclonal-activated ($CD44^{hi}$) or LCMV antigen–specific ($GP33^+$) $CD8^+$ effector T cells (bars represent samples sorted from cells pooled from at least three individual animals). ▲, PCR signal < 0.001; ◆, PCR signal below detection threshold.

Published October 6, 2009

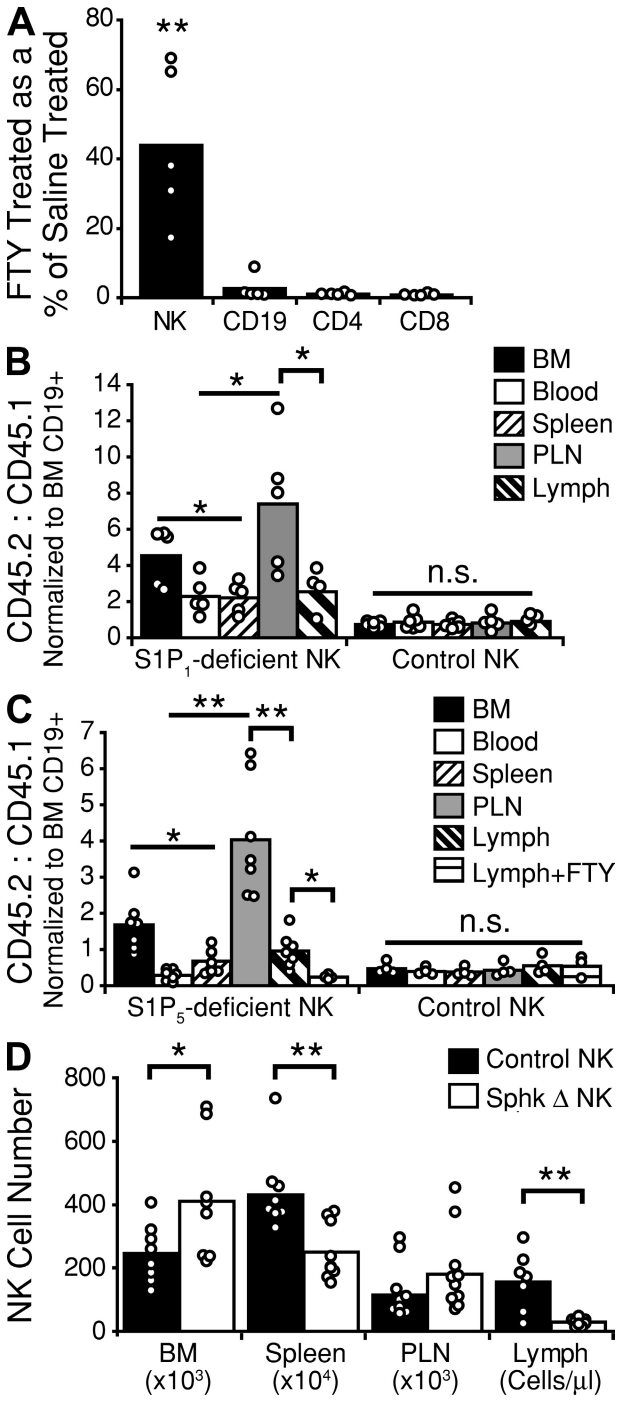

Figure 4. NK cell egress requires S1P, and uses both $S1P_5$ and an FTY720-sensitive receptor. (A) Cellular composition of lymph collected from wild-type mice treated for 20 h with 1 mg/kg FTY720. Values are reported as the number of cells in the lymph of FTY720-treated animals as a percentage of lymph cell numbers in saline-treated animals. Data are derived from at least three independent experiments. (B) Examination of wild-type B6 mice reconstituted with a mix of CD45.1$^+$ wild-type and CD45.2$^+$ *S1pr1*$^{-/-}$ or control *S1pr1*$^{+/+}$ BM. Values are reported as a ratio of $S1P_1$-deficient or control (CD45.2) to wild-type (CD45.1) cells. To account for differences between independent groups of chimeras, NK cell ratios were normalized to BM CD19$^+$ B cell ratios for each mouse. Data are derived from at least three independent experiments. (C) Examination of wild-type B6 mice reconstituted with a mix of CD45.1$^+$ wild-type and CD45.2$^+$ *S1pr5*$^{-/-}$ or CD45.2$^+$ *S1pr5*$^{+/+}$ littermate control BM. Some mice (Lymph+FTY) received 1 mg/kg FTY720 i.p. 20 h before analysis. Values are reported as a ratio of $S1P_5$-deficient or control (CD45.2) to wild-type (CD45.1) cells. NK cell ratios were normalized to BM CD19$^+$ B cell ratios for each mouse. Data are derived from two independent experiments. (D) Analysis of NK cell distribution in Sphk-deficient and littermate control mice. Values for BM, spleen, and peripheral LNs (six nodes) represent absolute NK cell numbers; values for lymph represent cells per microliter of lymph. Sphk Δ represents mice that were Sphk2 null, were deficient for one allele of *Sphk1*, and had the second allele of *Sphk1* excised. Control represents Sphk2-null mice with at least one functional allele of *Sphk1*. Data are derived from at least three independent experiments. Bars represent mean values, and circles represent individual animals. n.s., not significant; PLN, peripheral LN. *, $P \leq 0.05$; **, $P < 0.005$.

decay of T cell numbers, but NK cell numbers continued to decline (Fig. S4 A), indicating the presence of an FTY720-insensitive egress mechanism. Thus, FTY720 treatment appears to reduce but not block NK cell egress from LNs into lymph. To determine the impact of FTY720 exposure on S1P receptor expression, we examined the surface abundance of FLAG-tagged $S1P_1$ and $S1P_5$ in transduced WEHI-231 B lymphoma cells in the presence of either S1P or FTY720-P. As previously reported (Gonzalez-Cabrera et al., 2007; Oo et al., 2007), exposure to either S1P or FTY720-P, even in small quantities, was sufficient to induce loss of cell-surface $S1P_1$. Neither compound was able to affect the surface expression of $S1P_5$ (Fig. S4 B). The resistance of $S1P_5$ to down-modulation is unlikely to be caused by overexpression because the surface abundance of the receptor was lower than for $S1P_1$ (Fig. S4 B). These observations suggest that $S1P_5$ on lymphoid cells may be less sensitive than $S1P_1$ to agonist-mediated down-modulation.

The effects of FTY720 on T and B cell trafficking have been associated with intrinsic $S1P_1$ function in these cells (Matloubian et al., 2004). To determine if $S1P_1$ played a role in NK cell trafficking, mixed $S1P_1$-deficient and wild-type BM chimeras were examined (Fig. 4 B). Compared with control mixed chimeras, there was a small but significant accumulation of $S1P_1$-deficient NK cells in LNs compared with blood and spleen, and lower numbers of $S1P_1$-deficient NK cells in lymph (Fig. 4 B). There was also a mild accumulation of $S1P_1$-deficient cells in the BM. Thus, like FTY720 treatment, hematopoietic $S1P_1$ deficiency reduces but does not block NK cell egress from LNs into lymph.

To understand the role of $S1P_5$ in NK cell egress from lymphoid tissues, we generated $S1P_5$-deficient mice (Fig. S5). The $S1P_5$-deficient founders were backcrossed three times to B6 mice, and BM from either these mice or their $S1P_5^{+/+}$ littermates was used to generate mixed BM chimeras. These chimeras demonstrated a significant accumulation of $S1P_5$-deficient NK cells in the BM and in the LNs, together with a deficit of $S1P_5$-deficient NK cells in the blood and the spleen relative to wild-type NK cells (Fig. 4 C),

Published October 6, 2009

in agreement with previous findings (Walzer et al., 2007b). In addition, there was a lower ratio of $S1P_5$-deficient NK cells to wild-type NK cells in the lymph as compared with the peripheral LNs, indicating a reduced capacity of the $S1P_5$-deficient NK cells to egress from LNs into lymph. This ratio skewed further in favor of the wild-type NK cells if the mice were treated with FTY720 for 20 h before analysis (Fig. 4 C). These results indicate that $S1P_5$ is important for the egress of NK cells from LNs, while also indicating that some NK cell exit from LNs is $S1P_5$ independent and can be attributed to a receptor that is modulated by FTY720, most likely $S1P_1$.

To address the role of S1P in NK cell egress, we analyzed mice deficient in Sphk2 and conditionally ablated for *Sphk1*, and that lacked detectable circulatory S1P (Pappu et al., 2007). In these mice, we observed a significant reduction in the number of NK cells in the spleen but found these mice to have a normal or slightly elevated number of NK cells in peripheral LNs (Fig. 4 D). These mice also demonstrated a significant accumulation of NK cells in the BM. Analysis of lymph from these animals revealed a significant reduction in the number of NK cells, indicating a failure to egress from the peripheral lymphoid tissues in the absence of S1P (Fig. 4 D).

Reduced NK cell numbers in BM sinusoids of S1P-deficient mice

Cellular egress from the BM occurs via BM sinusoids. Recent work has shown that a 2-min in vivo exposure to PE-coupled anti-CD45 antibody selectively labels sinusoidal cells among BM cells (Pereira et al., 2009). Using this labeling procedure, we found that ~14% of BM NK cells were situated inside sinusoids (Fig. 5 A). In S1P-deficient mice, this frequency fell to <6% (Fig. 5 A). Previous studies have shown a tight relationship between $S1P_1$ surface abundance on T cells and local S1P concentrations (Lo et al., 2005; Schwab et al., 2005; Pappu et al., 2007). Analysis of T cells in the BM showed that $S1P_1$ was present in higher amounts on parenchymal compared with sinusoidal cells (Fig. 5 B), suggesting the existence of an increasing S1P gradient between parenchyma and sinusoid. These observations, coupled with the lower total NK cell numbers in the periphery, suggest that the ability of NK cells to exit from BM parenchyma to sinusoid is diminished in the absence of S1P.

$S1P_5$ mediates the egress of activated NK cells

CD69 is rapidly expressed at high levels on activated NK cells and may have a role in NK cell–mediated cytotoxicity (Karlhofer and Yokoyama, 1991). CD69 has also been shown to bind and inhibit the function of $S1P_1$ in T cell egress (Shiow et al., 2006). To test whether CD69 interacts with $S1P_5$, we used a coexpression system whereby a FLAG-tagged S1P receptor was coexpressed with a fusion molecule consisting of the extracellular and transmembrane domains of CD69 coupled to the intracellular domain of CD3ζ (Fig. S6). CD69 is known to physically associate with $S1P_1$, and cross-linking of FLAG-tagged $S1P_1$ results in the induction of CD3ζ signaling, as evident by the expression of an NFAT-regulated GFP reporter (Fig. 6 A). When FLAG-$S1P_5$ was cross-linked, no expression of GFP was detected, indicating a failure of CD69 to associate with $S1P_5$. Further, as previously reported (Shiow et al., 2006), immunoprecipitation of FLAG-$S1P_1$ resulted in the pull down of hemagglutinin (HA)-tagged CD69 (Fig. 6 B). Immunoprecipitation of FLAG-$S1P_5$, however, even from cells expressing higher amounts of the S1P receptor ($S1P_5$ ++ vs. $S1P_1$ +), failed to pull down any detectable HA-CD69 (Fig. 6 B). In agreement with the lack of interaction between CD69 and $S1P_5$, CD69 showed no ability to inhibit $S1P_5$-dependent S1P chemotaxis in Transwell assays with transduced cells (Fig. 6 C).

These observations suggested that, compared with T cells, NK cells may be resistant to LN egress inhibition caused by CD69 up-regulation. To assess the ability of CD69 to block NK egress in vivo, we analyzed the cellular composition of lymph from animals treated with the type I IFN–inducing agent poly I:C for 6 h. Treatment of mice with poly I:C has been previously demonstrated to efficiently block T cell

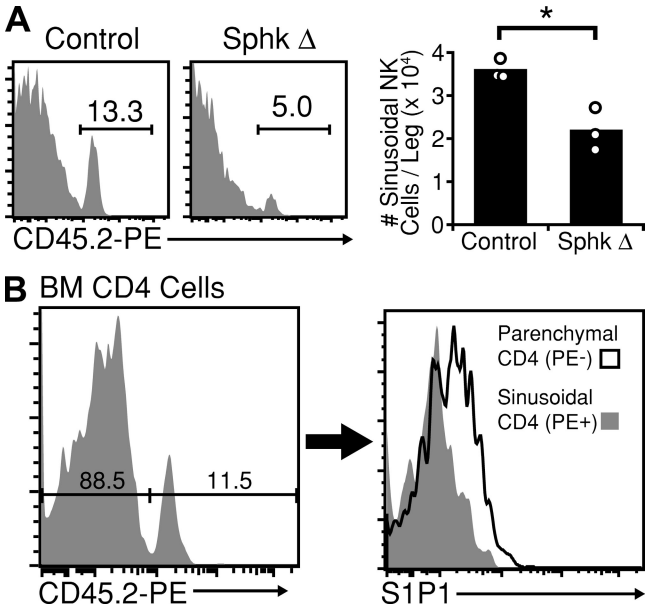

Figure 5. Reduced numbers of NK cells in BM sinusoids of S1P-deficient mice and $S1P_1$ surface expression on BM T cells. (A, left) NK cells present in the BM sinusoids of Sphk-deficient and littermate control mice were labeled in vivo by a 2-min i.v. treatment with PE-conjugated anti-CD45.2. Numbers indicate the frequency of PE^+ (sinusoidal) cells among total NK cells. (right) Summary of data for three mice. Data are representative of two independent experiments, each involving at least two Sphk-deficient and two littermate control mice. Bars represent mean values, and circles represent individual animals. (B, left) Control mice were treated i.v. with PE-conjugated anti-CD45.2 for 2 min. Cells were gated on $CD4^+$, $TCR\beta^+$, $NK1.1^-$ cells and resolved for sinusoidal labeling. (right) Comparison of $S1P_1$ surface expression levels between PE^- (parenchymal) and PE^+ (sinusoidal) $CD4^+$ T cells. Data are representative of two experiments, each analyzing two animals. *, $P < 0.05$.

Published October 6, 2009

egress from peripheral LNs (Shiow et al., 2006). Although nearly all T cell egress into lymph was inhibited by poly I:C treatment, a significant percentage of NK cells was found to retain the ability to enter the lymph (Fig. 6 D). Flow cytometric analysis confirmed that all NK cells in the lymph appeared activated and expressed high amounts of CD69 (Fig. 6 E), indicating that $S1P_5$ is able to mediate egress of activated NK cells even in the presence of CD69.

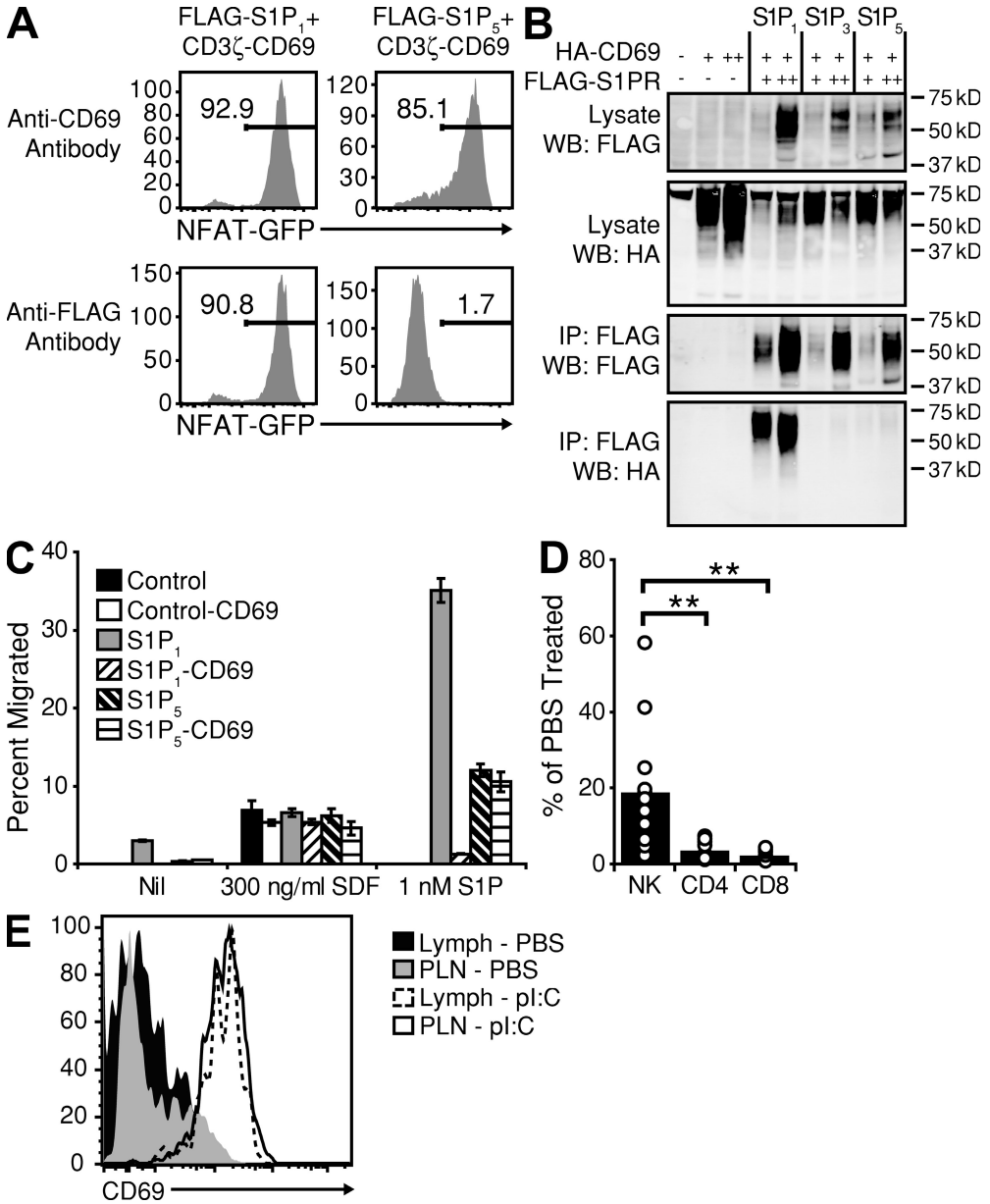

Figure 6. CD69 neither associates with nor inhibits $S1P_5$ function. (A) NFAT-GFP reporter expression in 2B4 cells transduced with the indicated constructs and treated with anti-CD69 antibody (top) or anti-FLAG antibody (bottom). Numbers indicate percentages of cells expressing the reporter. Data are representative of six independent experiments. (B) Western blot analysis of total lysates or anti-FLAG immunoprecipitates from WEHI-231 cells transduced with the indicated transgenes and sorted for CD69 and FLAG expression (+, low; ++, high). WB indicates the antibody used for Western blotting, and IP indicates the antibody used for immunoprecipitation. Data are representative of two independent experiments. (C) Transwell migration assay of untransduced WEHI-231 cells (control) or cells expressing S1PR transgenes alone or together with a CD69 transgene. Values are reported as the percentage of input cells migrating to the lower chamber during the 3-h assay. Columns represent the means of duplicate wells, and the bars represent the range within a single experiment. Data are representative of three independent experiments. (D) Cellular composition of lymph from animals treated with poly I:C for 6 h before analysis. Values are reported as the number of cells in the lymph of poly I:C–treated animals as the percentage of cells in the lymph of the PBS-treated animals. Data are representative of at least three independent experiments. Bars represent mean values, and circles represent individual animals. (E) Representative flow cytometric analysis of lymph and LN NK cells from saline- or poly I:C–treated mice. Data are representative of at least three independent experiments. PLN, peripheral LN. **, $P < 0.005$.

Published October 6, 2009

DISCUSSION

T-bet has been previously demonstrated to be important for normal NK cell development and survival (Townsend et al., 2004). NK cells from T-bet–deficient mice appear phenotypically immature and hyperactivated, and undergo increased rates of cell death. Although these observations may partly explain the observed deficit of NK cells in some peripheral sites of T-bet–deficient mice (blood, spleen, and liver), they do not explain the observed increase in NK cell number within the BM and peripheral LNs. Our findings indicate that $S1P_5$ is likely the key gene acting downstream of T-bet to allow the normal LN and BM egress of NK cells, and thus, recirculation to other sites. T-bet also promotes expression of CXCR3, a receptor involved in NK cell entry to inflamed LNs (Martín-Fontecha et al., 2004), indicating that part of the T-bet–induced gene expression program acts to coordinate NK cell trafficking. ChIP analysis identified the ability of T-bet to bind a conserved element 3′ of the *S1pr5* gene. This finding, together with our observation of T-bet–induced expression of $S1P_5$ in three different transduced cell types, as well as the T-bet dependence of $S1P_5$ expression in NK and $CD8^+$ T cells, establishes that $S1P_5$ is a common component of the T-bet gene expression program.

Within a day after activation in peripheral LNs, "primed" NK cells can be detected at distal sites such as the spleen, lungs, and liver (Lucas et al., 2007). This apparent ability of acutely activated NK cells to traffic from LNs seemed contrary to what has been observed for activated T cells, where CD69 inhibits $S1P_1$-mediated egress (Shiow et al., 2006). Our findings suggest that this is likely a consequence of $S1P_5$ being resistant to CD69-mediated inhibition. The expression of $S1P_5$ by effector $CD8^+$ T cells suggests that these cells may also be competent to egress while in an activated state. Similar trafficking patterns of NK cells and effector $CD8^+$ T cells have been noted (Grégoire et al., 2007). In this regard, it is notable that CD69 is a member of the NK receptor C-type lectin–like family, and some studies have suggested that it has an effector role (Karlhofer and Yokoyama, 1991), although no extrinsic ligand has yet been identified. By facilitating egress of $CD69^+$ cells, $S1P_5$ may allow this CD69 effector function to occur. Many iNKT cells express CD69 (Matsuda et al., 2000), and we propose that T-bet–induced $S1P_5$ also functions to facilitate egress and recirculation of these cells.

FTY720, in the active phosphorylated form, is a receptor agonist that is also a functional antagonist of $S1P_1$, and FTY720 treatment causes rapid down-modulation of $S1P_1$ on T cells, an effect that has correlated tightly with FTY720-mediated inhibition of T cell egress (Matloubian et al., 2004; Pham et al., 2008). In vitro studies have shown that FTY720-P causes internalization, ubiquitination, and degradation of $S1P_1$ (Gonzalez-Cabrera et al., 2007; Oo et al., 2007). In our studies, we found that in contrast to $S1P_1$, $S1P_5$ was resistant to FTY720-induced down-modulation, and our data suggest that this receptor continues to support NK cell egress in FTY720-treated hosts. The finding that NK cell egress is relatively, albeit not completely, resistant to FTY720 treatment is consistent with studies showing minimal changes in blood NK cell numbers in FTY720-treated humans (Vaessen et al., 2006) and mice (Walzer et al., 2007b). The ability of many NK cells to egress from LNs after FTY720 treatment provides further evidence against models arguing that FTY720 inhibits egress by acting on endothelial or stromal S1P receptors to close LN egress portals (Rosen and Goetzl, 2005). iNKT cell recirculation is also relatively resistant to FTY720 treatment (Allende et al., 2008). Our finding of $S1P_5$ expression in these T-bet–dependent cells provides a possible explanation for this finding, and it will be important in future studies to track the impact of $S1P_5$ deficiency on iNKT cell as well as NK cell and effector $CD8^+$ T cell function.

Although $S1P_5$ appears to be the dominant S1P receptor in NK cells, we did observe $S1P_1$ expression in these cells, and $S1P_1$ deficiency caused a measurable decrease in NK cell representation in lymph. Although a previous study suggested $S1P_1$ may not be present in NK cells (Walzer et al., 2007b), $S1P_1$ transcripts were within ~10-fold of the amounts present in T and B cells in that study, as observed in the present work. The greater effect of S1P deficiency than $S1P_5$ deficiency on NK cell numbers in lymph also supports the view that $S1P_1$ plays a role in these cells, as does the finding that FTY720 treatment is able to further reduce the egress of $S1P_5$–deficient NK cells. It remains to be determined whether these receptors are coexpressed in all NK cells or expressed in separate subsets.

Within the spleen, NK cells are largely excluded from the white pulp and are localized in the red pulp (Walzer et al., 2007a). $S1P_1$ deficiency or FTY720 treatment depletes T and B cells from red pulp while leaving cells within the white pulp. This likely reflects a role for S1P and $S1P_1$ in overcoming chemokine-mediated retention in the white pulp (Pham et al., 2008). The general NK cell deficiency in the spleen of T-bet–, $S1P_5$–, and S1P-deficient mice is consistent with observations that few splenic NK cells are present within the white pulp, and with evidence that positioning in the red pulp is $G_{\alpha i}$ independent and, thus, most likely not chemokine mediated (Grégoire et al., 2007). The lack of a $G_{\alpha i}$ mediated retention mechanism may well obviate the need for S1P receptor signaling during splenic egress (Pham et al., 2008). We suspect that in the absence of $S1P_5$ or S1P, NK cells become trapped in LNs and BM at the expense of representation in blood and the splenic red pulp. We note that the reduction in NK cell numbers in the spleens and livers of T-bet–deficient mice exceeds their numerical accumulation in LNs and BM, likely reflecting a requirement for T-bet in the maturation or maintenance of NK cells. Although T-bet has a large number of target genes, there may be a similar deficiency in the total peripheral NK cell pool in $S1P_5$–deficient mice (Walzer et al., 2007b), raising the possibility that T-bet–driven $S1P_5$ expression is required for normal NK cell maturation or homeostasis, a topic that will need further assessment in future studies.

The requirements for cell egress from the BM are poorly understood. CXCR4 has an established role in mediating precursor retention in the BM and there is evidence that

Published October 6, 2009

NK cells are retained by CXCR4, and down-regulation of this receptor coincides with maturation and exit from the BM (Beider et al., 2003; Bernardini et al., 2008). However, mature NK cells retain substantial amounts of CXCR4 and are highly responsive to CXCL12 (Bernardini et al., 2008). We suggest that the requirement for S1P for efficient egress of NK cells from BM parenchyma into sinusoids reflects a role for S1P, together with $S1P_5$ and $S1P_1$, in overcoming CXCR4–CXCL12–mediated retention, analogously to S1P–$S1P_1$ overcoming the CCR7–CCL21–mediated retention of T cells in lymph nodes (Pham et al., 2008). These findings point to the possibility that S1P and S1P receptors function in the BM egress of additional cell types. This has important implications for the application of therapies that interrupt S1P receptor function.

In summary, our findings establish that T-bet promotes $S1P_5$ expression and that $S1P_5$, and its ligand S1P, are required for NK cell egress from LNs and BM. T-bet–dependent $S1P_5$ expression also occurs in effector $CD8^+$ T cells. These findings extend the paradigm that S1P promotes egress through actions on migrating $S1P_1{}^+$ cells by showing that a second leukocyte S1P receptor is involved in egress. We propose that the differential use of $S1P_5$ by NK and effector $CD8^+$ T cells facilitates their egress in a $CD69^+$ effector state. Finally, our study adds to recent findings (Walzer et al., 2007b) to suggest strongly that S1P and S1P receptors are required for efficient NK cell egress from the BM.

MATERIALS AND METHODS

Mice, ENU mutagenesis, chimeras, lymphocyte transfers, and treatments. C57BL/6 (B6) and CD45.1-congenic B6 mice were obtained from the National Cancer Institute (NCI). C57BL/10 and CBA/J mice were obtained from the Australian Phenomics Facility, Australian National University (ANU). *Tbx21*$^{-/-}$ mice were obtained from the Jackson Laboratory. All experiments conformed to ethical principles and guidelines approved by the University of California, San Francisco Institutional Animal Care and Use Committee, the ANU Animal Experimentation Ethics Committee, and the Scripps Research Institute Animal Research Committee. The generation of $S1P_5$-deficient mice is described in detail in the following section. $S1P_5$-deficient mice were crossed three times to B6 mice. The generation of $S1P_1$-deficient mice, $S1P_1$-deficient fetal liver chimeras, and Sphk-deficient mice have been previously described (Liu et al., 2000; Matloubian et al., 2004; Pappu et al., 2007). S1P1$^{+/-}$ mice were provided by R. Proia (National Institute of Diabetes and Digestive and Kidney Diseases, Bethesda, MD), and Sphk1$^{f/-}$ Sphk2$^{-/-}$ mice were provided by S. Coughlin (University of California, San Francisco, San Francisco, CA). The Duane strain was established through ENU-mediated mutagenesis of B6 mice, as previously described (Nelms and Goodnow, 2001; Shiow et al., 2008). Mapping and sequencing of the Duane mutation was performed at the Australian Cancer Research Foundation (ACRF) Biomolecular Resource Facility (John Curtin School of Medical Research [JCSMR], ANU) and is described in Genetic mapping of the Duane mutation. Once identified, the Duane strain was backcrossed onto B6 mice for three additional generations. BM chimeras were generated by i.v. transferring 3–6 × 10^6 BM cells into lethally irradiated (2 × 550 rads) B6-CD45.1 recipients.

For short-term adoptive transfers of splenocytes, 2.5–3.5 × 10^7 donor cells were transferred i.v. into each B6-CD45.1 recipient. Integrin and L-selectin blockade was mediated by the administration of 100 μg each of anti–αL integrin (clone M17/4), anti–α4 integrin (clone PS/2), and anti–L-selectin (clone MEL14) antibodies in PBS i.v. 40 h before analysis. FTY720-treated animals received 1 mg/kg of the drug injected i.p. and were analyzed 20–24 h later. For in vivo lymphocyte activation, mice received 100 μg of poly I:C (GE Healthcare) in PBS i.v. 6 h before analysis. Lymph collection and in vivo labeling of BM sinusoidal contents have been previously described (Matloubian et al., 2004; Pereira et al., 2009). For isolation of liver NK cells, livers were harvested and rinsed in PBS. The liver was disrupted by forcing through a 70-μm nylon mesh, and cells were washed in PBS, resuspended in 44% Percoll (GE Healthcare) and layered on 56% Percoll. Preparations were spun for 20 min at 2,000 rpm in a bench-top centrifuge with no brake, after which the interface containing the lymphocytes was collected and washed in PBS. Lymphocytic choriomeningitis (LCMV) infections were performed as previously described (Intlekofer et al., 2008), and $CD44^{hi}$ $CD8^+$ T cells were sorted on day 8 after infection from total splenocytes.

***S1pr5* targeting vector construction, embryonic stem (ES) cell manipulation, and generation of mutant mice.** A mouse genomic library was screened with an $S1P_5$ mouse cDNA, and an S1pr5-containing genomic clone with sufficient flanking sequence on both sides of the $S1P_5$ coding region was identified. The *S1pr5* targeting construct in pBluescript (Agilent Technologies) has an ∼2.6-kb short arm and an ∼3.2-kb long arm, and a portion of the $S1P_5$ coding region was fused with DsRed from DSRed-N1 (Takara Bio Inc.). Except for the first seven amino acids, the entire $S1P_5$ coding region was deleted. The orientation of the neomycin cassette under the control of the phosphogylcerate kinase promoter is opposite to that of the *S1pr5* genomic locus. All cloning was performed using standard molecular biology techniques.

E14Tg2a stem cells were electroporated with 25 μg of Sal I–linearized targeting vector at the Scripps Research Institute Mouse Genetics Core, and ∼150 colonies were isolated. Genomic DNA was prepared from isolated stem cells digested with BamHI and Southern blotted with a random-primed ^{32}P-labeled external probe. Two independent ES cell clones with recombined *S1pr5* loci were identified and injected into blastocysts. One line of chimeric mice derived from the identified ES cell clones transmitted the mutant allele to the germline. The resultant heterozygous mice were crossed, and the presence of wild-type, heterozygous, and null mutants was confirmed by Southern blotting of BamHI-digested tail DNA with the external probe, and PCR using $S1P_5$- and DsRed-specific primers (Table S1). PCR was performed under standard conditions, except for the addition of 10% DMSO (final) to reaction mixes.

Genetic mapping of the Duane mutation. Affected Duane mice were crossed onto either the C57BL/10 or the CBA/J background to generate heterozygous F1 mice. These F1 mice were either intercrossed (C57BL/10 mapping) or backcrossed to an affected Duane mouse (CBA/J mapping) to yield mice homozygous for the Duane mutation and carrying a mix of C57BL/6 and background C57BL/10 or CBA/J SNPs. Genomic DNA was isolated from both affected and unaffected mice from the C57BL10/mapping cross and was used as template material for SNP mapping using an Amplifluor assay (Millipore) with Platinum Taq (Invitrogen). SNP markers were spaced approximately every 20 Mbp throughout the genome. To confirm the linkage and to further narrow the interval, genomic DNA from both affected and unaffected mice from the CBA/J mapping cross was isolated and used as a template material for SNP typing in the suspected interval. Once a defined interval was established, the T-bet–encoding gene was sequenced from genomic DNA from both affected Duane and wild-type mice. All exons were amplified by PCR with primers (Table S1) spanning the whole exon and the flanking intronic regions. To confirm the transcript sequence, RNA was isolated with TRIzol reagent (Invitrogen) from mutant, heterozygous, and wild-type mice, and cDNA was synthesized with the SuperScript II reverse transcription kit (Invitrogen). The Duane deletion was confirmed with primers located in exons 2 and 4 (Table S1). All PCR products were amplified by using AccuPrime High Fidelity Taq (Invitrogen), gel purified, and sequenced on a sequencer (ABI 3730; Applied Biosytems) at the ACRF Biomolecular Resource Facility (JCSMR, ANU) according to the manufacturer's protocol.

Protein modeling. T-bet protein models were generated by using the Geno3D server (available at http://geno3d-pbil.ibcp.fr; Combet et al., 2002).

Published October 6, 2009

Resulting models were visualized and colored using the DeepView: Swiss-PdbViewer software package (available at http://www.expasy.org/spdbv/; Guex and Peitsch, 1997). Final images were rendered with the Persistence of Vision Raytracer (POV-Ray, version 3.6.1a; Hallam Oaks Pty. Ltd.).

Cell-culture conditions. For polyclonal T cell stimulation, splenocytes were first depleted of $B220^+$, $NK1.1^+$, $CD11b^+$, $CD11c^+$, and $Gr1^+$ cells by using a cell separator (autoMACS; Miltenyi Biotec). The remaining T cells were resuspended in RPMI Complete (RPMI 1640 [Cellgro] supplemented with 10% FBS [Invitrogen], 10 mM Hepes [Cellgro], 100 U/ml penicillin–streptomycin [Thermo Fisher Scientific], and 50 μM 2-mercaptoethanol) and were plated at 2.5×10^6 cells/ml in 24-well plates precoated with 3 μg/ml anti-CD3 (clone 2C11) and 0.5 μg/ml anti-CD28 (clone 37.51). After 48 h of culture, cells were harvested for flow cytometric and immunoblotting analysis.

Isotype class switch assays were performed with total splenocytes. Cells were resuspended in RPMI Complete supplemented with 5 μg/ml $F(ab')^2$ goat anti–mouse IgM (Jackson ImmunoResearch Laboratories), 100 μg/ml IFN-γ (R&D Systems), and 20 μg/ml LPS (Sigma) and were plated at 2.5×10^5 cells/ml in 24-well plates. Fresh media was added to the cultures after 48 h, and cells were harvested for flow cytometric analysis after 96 h.

For Th1 cell differentiation assays, total splenocytes were cultured in T cell media (Iscove's medium [Cellgro] with 10% FBS, 1 mM sodium pyruvate, 100 U/ml penicillin–streptomycin, 2.5 μM 2-mercaptoethanol, and 20 U/ml human IL-2 [NCI Preclinical Repository]) supplemented with 20 ng/ml of mouse IL-12 (R&D Systems), 10 μg/ml anti–IL-4 (clone 11B.11), 0.5 μg/ml anti-CD3 (clone 2C11), and 2 μg/ml anti-CD28 (clone 37.51). Cells were resuspended at 3×10^6 cells/ml and cultured in 24-well plates. After 72 h, cultures were transferred into 6-well plates and supplemented with fresh T cell media supplemented with IL-2, IL-12, and anti–IL-4, and then cultured for an additional 48 h. Before flow cytometric analysis, cells were stimulated with 100 ng/ml PMA (Sigma-Aldrich) and 2 μg/ml ionomycin (EMD) for 3 h in the presence of GolgiPlug (BD). $CD8^+$ effector T cells were generated by A. Intlekofer (University of Pennsylvania, Philadelphia, PA), as previously described (Intlekofer et al., 2005).

Quantitative PCR. For quantitative PCR, total RNA was isolated from frozen cell pellets with the RNeasy Micro Kit (QIAGEN) or from freshly dissected spinal cords with TRIzol reagent. cDNA was synthesized from cell pellets by using Moloney murine leukemia virus (Invitrogen) or from DNase-treated spinal cord RNA by using SuperScript II reverse transcription, and served as a template for subsequent amplifications using either 2× SYBR Green (Roche) or AmpliTaqGold (Applied Biosystems) PCR kits. Samples were analyzed using an ABI 7300 (Applied Biosystems).

Retroviral vector constructs and transductions. Construction of an MSCV2.2 retroviral vector containing a FLAG-tagged mouse $S1P_1$, IRES, and a truncated human CD4 (hCD4) has been previously described (Lo et al., 2005). MSCV2.2 vector constructs containing FLAG-tagged mouse $S1P_5$, wild-type mouse T-bet, and Duane T-bet upstream of the IRES hCD4 elements were generated in a similar fashion. The generation of MSCV2.2 vectors containing HA-tagged mouse CD69 or a chimeric molecule of the extracellular and transmembrane domains of mouse CD69 and the cytoplasmic domain of human CD3ζ upstream of an IRES and GFP element has been described previously (Shiow et al., 2006). These vectors were used to transfect Bosc23 packaging cells, and supernatants containing infectious viral particles were collected as previously described (Lo et al., 2005). Retroviruses were subsequently used to spinfect WEHI-231 and 2B4 cells. For Western blotting and quantitative PCR analysis of T-bet overexpression in WEHI-231 cells, equal numbers of cells gated for equivalent expression of the hCD4 reporter were sorted for each transduction by using a FACSAria (BD) and snap frozen in liquid nitrogen. Transduction of primary T cells was performed as previously described (Intlekofer et al., 2005), and GFP^+ cells were sorted for quantitative PCR analysis and snap frozen.

Immunoprecipitation and Western blotting. Immunoprecipitation was performed as previously described (Shiow et al., 2006). For immunoblot analysis, cell pellets were lysed in 0.875% Brij97, 0.125% NP-40, 150 mM NaCl, 10 mM Tris-HCl (pH 7.4), and 0.02% NaN_3 buffer containing protease inhibitors (Sigma-Aldrich). Samples were resolved by 10% SDS-PAGE (NuPAGE; Invitrogen) and transferred to Immobilon-FL membranes (Millipore). Membranes were blocked with buffer (LI-COR Biosciences) and stained with anti–T-bet (clone 39D raised against full-length mouse T-bet; Santa Cruz Biotechnology, Inc.), rabbit anti-actin (Sigma-Aldrich), anti-FLAG (clone M1; Sigma-Aldrich), and biotin-conjugated anti-HA (clone 3F10; Roche). Products were detected with IRDye 680–conjugated goat anti–mouse Ig, IRDye 800CW–conjugated streptavidin (LI-COR Biosciences), or IRDye 700DX–conjugated donkey anti–rabbit Ig (Rockland), and imaged on an infrared imager (Odyssey; LI-COR Biosciences).

ChIP. ChIP was performed as previously described (Miller et al., 2008). Primers specific to the 3′ region of the *S1pr5* gene were as follows: forward, 5′-CACCTTGCAGTAGCTCTGAG-3′, and reverse, 5′-GGAGCCAGCCGGACTGTATC-3′.

Luciferase reporter and endogenous T-bet target transcription analyses. Luciferase and endogenous gene quantitative RT-PCR analyses were performed as previously described (Miller et al., 2008).

NFAT-GFP reporter assay. S1P receptor and CD69–hCD3ζ fusion proteins were cotransduced into mouse 2B4 hybridoma cells with an NFAT-GFP reporter construct and were assayed as previously described (Arase et al., 2002; Rosen et al., 2005; Shiow et al., 2006).

S1PR down-modulation assay. WEHI-231 cells stably expressing FLAG-tagged S1PR were washed twice in RPMI 1640 medium with 10 mM Hepes and 0.5% fatty acid–free BSA (EMD; BSA-RPMI), and then incubated in BSA-RPMI for 30 min at 37°C. S1PR ligands indicated in the figures (S1P or FTY720-P) were titrated into BSA-RPMI in a 96-well U-bottom plate. Cells were added to each well, and the plate was incubated for 40 min at 37°C. The resulting surface S1PR levels were measured by flow cytometry using the anti-FLAG antibody (clone M2; Sigma-Aldrich).

Transwell migration. Transwell migrations were performed as previously described (Matloubian et al., 2004; Lo et al., 2005). In brief, transduced WEHI-231 cells were harvested, washed, and incubated for 30 min at 37°C in migration media (RPMI 1640 supplemented with 10 mM Hepes, 100 U/ml penicillin–streptomycin, and 0.5% fatty acid–free BSA). 10^6 cells were loaded into 5-μm Transwells (Sigma-Aldrich) and allowed to transmigrate for 3 h in response to media alone, stromal cell–derived factor 1 (PeproTech), or S1P (Sigma-Aldrich). Contents from the bottom of each well were harvested and enumerated by flow cytometry.

Online supplemental material. Table S1 lists nucleotide sequences for PCR primer and probe sets. Fig. S1 contains representative flow cytometric analysis and NK cell counts from various tissues from Duane and wild-type mice. Fig. S2 presents mapping and nucleotide sequencing of the causative genetic lesion within the Duane *Tbx21* gene, amplification and sequencing of Duane and wild-type T-bet cDNA, and quantitative PCR and Western blot analysis of T-bet expression in Duane and wild-type mice. Fig. S3 presents assays demonstrating that the Duane T-bet mutation results in a functionally null phenotype. Fig. S4 contains analysis of NK cell numbers in peripheral LNs from mice after blocking lymphocyte entry in the presence or absence of FTY720, and representative flow cytometric analysis of untreated and S1P- or FTY720-treated 2B4 hybridoma cells transduced with either FLAG-$S1P_1$ or FLAG-$S1P_5$. Fig. S5 illustrates the generation of $S1P_5$-deficient mice. Fig. S6 presents representative cell-surface staining for CD69 and FLAG on transduced 2B4 hybridoma cells used for NFAT-GFP reporter assays. Online supplemental material is available at http://www.jem.org/cgi/content/full/jem.20090525/DC1.

We thank S. Coughlin and R. Proia for mice; A. Intlekofer for the CD8+ effector T cells; A. Yang for generation of the *S1pr5* targeting construct; J. Green, T. Pham, and B. Whittle for technical advice; and J. An for expert animal husbandry.

A. Enders was supported by a Deutsche Forschungsgemeinschaft Research Fellowship (EN 790/1-1) and the Ramaciotti Foundation. A.S. Weinmann is supported by grants from the National Institute of Allergy and Infectious Disease (AI061061) and the American Cancer Society. S.A. Miller is supported by a predoctoral training grant from the National Institute of General Medical Sciences (T3207270). C.C. Goodnow was supported by the Ramaciotti Foundation and is an Australian Research Council Federation Fellow. L.L. Lanier is an American Cancer Society Research Professor. J.G. Cyster is an investigator of the Howard Hughes Medical Institute. This work was supported by grants from the National Institutes of Health (AI52127, BAA-NIH-NIAID-DAIT-07-35, AI74847, and DA019674).

The authors have no financial conflicts of interest.

Submitted: 6 March 2009
Accepted: 8 September 2009

REFERENCES

Allende, M.L., J.L. Dreier, S. Mandala, and R.L. Proia. 2004. Expression of the sphingosine 1-phosphate receptor, S1P1, on T-cells controls thymic emigration. *J. Biol. Chem.* 279:15396–15401. doi:10.1074/jbc.M314291200

Allende, M.L., D. Zhou, D.N. Kalkofen, S. Benhamed, G. Tuymetova, C. Borowski, A. Bendelac, and R.L. Proia. 2008. S1P1 receptor expression regulates emergence of NKT cells in peripheral tissues. *FASEB J.* 22:307–315. doi:10.1096/fj.07-9087com

Arase, H., E.S. Mocarski, A.E. Campbell, A.B. Hill, and L.L. Lanier. 2002. Direct recognition of cytomegalovirus by activating and inhibitory NK cell receptors. *Science.* 296:1323–1326. doi:10.1126/science.1070884

Bajénoff, M., B. Breart, A.Y. Huang, H. Qi, J. Cazareth, V.M. Braud, R.N. Germain, and N. Glaichenhaus. 2006. Natural killer cell behavior in lymph nodes revealed by static and real-time imaging. *J. Exp. Med.* 203:619–631. doi:10.1084/jem.20051474

Barrett, T., D.B. Troup, S.E. Wilhite, P. Ledoux, D. Rudnev, C. Evangelista, I.F. Kim, A. Soboleva, M. Tomashevsky, and R. Edgar. 2007. NCBI GEO: mining tens of millions of expression profiles–database and tools update. *Nucleic Acids Res.* 35:D760–D765. doi:10.1093/nar/gkl887

Beider, K., A. Nagler, O. Wald, S. Franitza, M. Dagan-Berger, H. Wald, H. Giladi, S. Brocke, J. Hanna, O. Mandelboim, et al. 2003. Involvement of CXCR4 and IL-2 in the homing and retention of human NK and NK T cells to the bone marrow and spleen of NOD/SCID mice. *Blood.* 102:1951–1958. doi:10.1182/blood-2002-10-3293

Beima, K.M., M.M. Miazgowicz, M.D. Lewis, P.S. Yan, T.H. Huang, and A.S. Weinmann. 2006. T-bet binding to newly identified target gene promoters is cell type-independent but results in variable context-dependent functional effects. *J. Biol. Chem.* 281:11992–12000. doi:10.1074/jbc.M513613200

Bernardini, G., G. Sciumè, D. Bosisio, S. Morrone, S. Sozzani, and A. Santoni. 2008. CCL3 and CXCL12 regulate trafficking of mouse bone marrow NK cell subsets. *Blood.* 111:3626–3634. doi:10.1182/blood-2007-08-106203

Bult, C.J., J.T. Eppig, J.A. Kadin, J.E. Richardson, and J.A. Blake; Mouse Genome Database Group. 2008. The Mouse Genome Database (MGD): mouse biology and model systems. *Nucleic Acids Res.* 36:D724–D728. doi:10.1093/nar/gkm961

Chen, S., H. Kawashima, J.B. Lowe, L.L. Lanier, and M. Fukuda. 2005. Suppression of tumor formation in lymph nodes by L-selectin–mediated natural killer cell recruitment. *J. Exp. Med.* 202:1679–1689. doi:10.1084/jem.20051473

Chen, G.Y., H. Osada, L.F. Santamaria-Babi, and R. Kannagi. 2006. Interaction of GATA-3/T-bet transcription factors regulates expression of sialyl Lewis X homing receptors on Th1/Th2 lymphocytes. *Proc. Natl. Acad. Sci. USA.* 103:16894–16899. doi:10.1073/pnas.0607926103

Combet, C., M. Jambon, G. Deléage, and C. Geourjon. 2002. Geno3D: automatic comparative molecular modelling of protein. *Bioinformatics.* 18:213–214. doi:10.1093/bioinformatics/18.1.213

Djuretic, I.M., D. Levanon, V. Negreanu, Y. Groner, A. Rao, and K.M. Ansel. 2007. Transcription factors T-bet and Runx3 cooperate to activate Ifng and silence Il4 in T helper type 1 cells. *Nat. Immunol.* 8:145–153. doi:10.1038/ni1424

Garrod, K.R., S.H. Wei, I. Parker, and M.D. Cahalan. 2007. Natural killer cells actively patrol peripheral lymph nodes forming stable conjugates to eliminate MHC-mismatched targets. *Proc. Natl. Acad. Sci. USA.* 104:12081–12086. doi:10.1073/pnas.0702867104

Gonzalez-Cabrera, P.J., T. Hla, and H. Rosen. 2007. Mapping pathways downstream of sphingosine 1-phosphate subtype 1 by differential chemical perturbation and proteomics. *J. Biol. Chem.* 282:7254–7264. doi:10.1074/jbc.M610581200

Gräler, M.H., and E.J. Goetzl. 2004. The immunosuppressant FTY720 down-regulates sphingosine 1-phosphate G-protein-coupled receptors. *FASEB J.* 18:551–553.

Grégoire, C., L. Chasson, C. Luci, E. Tomasello, F. Geissmann, E. Vivier, and T. Walzer. 2007. The trafficking of natural killer cells. *Immunol. Rev.* 220:169–182. doi:10.1111/j.1600-065X.2007.00563.x

Guex, N., and M.C. Peitsch. 1997. SWISS-MODEL and the Swiss-PdbViewer: an environment for comparative protein modeling. *Electrophoresis.* 18:2714–2723. doi:10.1002/elps.1150181505

Gustafsson, K., M. Ingelsten, L. Bergqvist, J. Nyström, B. Andersson, and A. Karlsson-Parra. 2008. Recruitment and activation of natural killer cells in vitro by a human dendritic cell vaccine. *Cancer Res.* 68:5965–5971. doi:10.1158/0008-5472.CAN-07-6494

Hwang, E.S., S.J. Szabo, P.L. Schwartzberg, and L.H. Glimcher. 2005. T helper cell fate specified by kinase-mediated interaction of T-bet with GATA-3. *Science.* 307:430–433. doi:10.1126/science.1103336

Intlekofer, A.M., N. Takemoto, E.J. Wherry, S.A. Longworth, J.T. Northrup, V.R. Palanivel, A.C. Mullen, C.R. Gasink, S.M. Kaech, J.D. Miller, et al. 2005. Effector and memory CD8+ T cell fate coupled by T-bet and eomesodermin. *Nat. Immunol.* 6:1236–1244. doi:10.1038/ni1268

Intlekofer, A.M., A. Banerjee, N. Takemoto, S.M. Gordon, C.S. Dejong, H. Shin, C.A. Hunter, E.J. Wherry, T. Lindsten, and S.L. Reiner. 2008. Anomalous type 17 response to viral infection by CD8+ T cells lacking T-bet and eomesodermin. *Science.* 321:408–411. doi:10.1126/science.1159806

Joshi, N.S., W. Cui, A. Chandele, H.K. Lee, D.R. Urso, J. Hagman, L. Gapin, and S.M. Kaech. 2007. Inflammation directs memory precursor and short-lived effector CD8(+) T cell fates via the graded expression of T-bet transcription factor. *Immunity.* 27:281–295. doi:10.1016/j.immuni.2007.07.010

Karlhofer, F.M., and W.M. Yokoyama. 1991. Stimulation of murine natural killer (NK) cells by a monoclonal antibody specific for the NK1.1 antigen. IL-2-activated NK cells possess additional specific stimulation pathways. *J. Immunol.* 146:3662–3673.

Kassim, S.H., N.K. Rajasagi, B.W. Ritz, S.B. Pruett, E.M. Gardner, R. Chervenak, and S.R. Jennings. 2009. Dendritic cells are required for optimal activation of natural killer functions following primary infection with herpes simplex virus type 1. *J. Virol.* 83:3175–3186. doi:10.1128/JVI.01907-08

Lewis, M.D., S.A. Miller, M.M. Miazgowicz, K.M. Beima, and A.S. Weinmann. 2007. T-bet's ability to regulate individual target genes requires the conserved T-box domain to recruit histone methyltransferase activity and a separate family member-specific transactivation domain. *Mol. Cell. Biol.* 27:8510–8521. doi:10.1128/MCB.01615-07

Liu, Y., R. Wada, T. Yamashita, Y. Mi, C.X. Deng, J.P. Hobson, H.M. Rosenfeldt, V.E. Nava, S.S. Chae, M.J. Lee, et al. 2000. Edg-1, the G protein-coupled receptor for sphingosine-1-phosphate, is essential for vascular maturation. *J. Clin. Invest.* 106:951–961. doi:10.1172/JCI10905

Lo, C.G., Y. Xu, R.L. Proia, and J.G. Cyster. 2005. Cyclical modulation of sphingosine-1-phosphate receptor 1 surface expression during lymphocyte recirculation and relationship to lymphoid organ transit. *J. Exp. Med.* 201:291–301. doi:10.1084/jem.20041509

Lucas, M., W. Schachterle, K. Oberle, P. Aichele, and A. Diefenbach. 2007. Dendritic cells prime natural killer cells by trans-presenting interleukin 15. *Immunity.* 26:503–517. doi:10.1016/j.immuni.2007.03.006

Lugo-Villarino, G., R. Maldonado-Lopez, R. Possemato, C. Penaranda, and L.H. Glimcher. 2003. T-bet is required for optimal production of IFN-gamma and antigen-specific T cell activation by dendritic cells. *Proc. Natl. Acad. Sci. USA.* 100:7749–7754. doi:10.1073/pnas.1332767100

Mandala, S., R. Hajdu, J. Bergstrom, E. Quackenbush, J. Xie, J. Milligan, R. Thornton, G.J. Shei, D. Card, C. Keohane, et al. 2002. Alteration

of lymphocyte trafficking by sphingosine-1-phosphate receptor agonists. *Science*. 296:346–349. doi:10.1126/science.1070238

Martín-Fontecha, A., L.L. Thomsen, S. Brett, C. Gerard, M. Lipp, A. Lanzavecchia, and F. Sallusto. 2004. Induced recruitment of NK cells to lymph nodes provides IFN-gamma for T(H)1 priming. *Nat. Immunol.* 5:1260–1265. doi:10.1038/ni1138

Matloubian, M., C.G. Lo, G. Cinamon, M.J. Lesneski, Y. Xu, V. Brinkmann, M.L. Allende, R.L. Proia, and J.G. Cyster. 2004. Lymphocyte egress from thymus and peripheral lymphoid organs is dependent on S1P receptor 1. *Nature*. 427:355–360. doi:10.1038/nature02284

Matsuda, J.L., O.V. Naidenko, L. Gapin, T. Nakayama, M. Taniguchi, C.R. Wang, Y. Koezuka, and M. Kronenberg. 2000. Tracking the response of natural killer T cells to a glycolipid antigen using CD1d tetramers. *J. Exp. Med.* 192:741–754. doi:10.1084/jem.192.5.741

Mehta, D.S., A.L. Wurster, A.S. Weinmann, and M.J. Grusby. 2005. NFATc2 and T-bet contribute to T-helper-cell-subset-specific regulation of IL-21 expression. *Proc. Natl. Acad. Sci. USA*. 102:2016–2021. doi:10.1073/pnas.0409512102

Miller, S.A., A.C. Huang, M.M. Miazgowicz, M.M. Brassil, and A.S. Weinmann. 2008. Coordinated but physically separable interaction with H3K27-demethylase and H3K4-methyltransferase activities are required for T-box protein-mediated activation of developmental gene expression. *Genes Dev.* 22:2980–2993. doi:10.1101/gad.1689708

Nelms, K.A., and C.C. Goodnow. 2001. Genome-wide ENU mutagenesis to reveal immune regulators. *Immunity*. 15:409–418. doi:10.1016/S1074-7613(01)00199-6

Oo, M.L., S. Thangada, M.T. Wu, C.H. Liu, T.L. Macdonald, K.R. Lynch, C.Y. Lin, and T. Hla. 2007. Immunosuppressive and anti-angiogenic sphingosine 1-phosphate receptor-1 agonists induce ubiquitinylation and proteasomal degradation of the receptor. *J. Biol. Chem.* 282:9082–9089. doi:10.1074/jbc.M610318200

Pappu, R., S.R. Schwab, I. Cornelissen, J.P. Pereira, J.B. Regard, Y. Xu, E. Camerer, Y.W. Zheng, Y. Huang, J.G. Cyster, and S.R. Coughlin. 2007. Promotion of lymphocyte egress into blood and lymph by distinct sources of sphingosine-1-phosphate. *Science*. 316:295–298. doi:10.1126/science.1139221

Peng, S.L., S.J. Szabo, and L.H. Glimcher. 2002. T-bet regulates IgG class switching and pathogenic autoantibody production. *Proc. Natl. Acad. Sci. USA*. 99:5545–5550. doi:10.1073/pnas.082114899

Pereira, J.P., J. An, Y. Xu, Y. Huang, and J.G. Cyster. 2009. Cannabinoid receptor 2 mediates the retention of immature B cells in bone marrow sinusoids. *Nat. Immunol.* 10:403–411.

Pham, T.H., T. Okada, M. Matloubian, C.G. Lo, and J.G. Cyster. 2008. S1P1 receptor signaling overrides retention mediated by G alpha i-coupled receptors to promote T cell egress. *Immunity*. 28:122–133. doi:10.1016/j.immuni.2007.11.017

Rosen, H., and E.J. Goetzl. 2005. Sphingosine 1-phosphate and its receptors: an autocrine and paracrine network. *Nat. Rev. Immunol.* 5:560–570. doi:10.1038/nri1650

Rosen, D.B., J. Bettadapura, M. Alsharifi, P.A. Mathew, H.S. Warren, and L.L. Lanier. 2005. Cutting edge: lectin-like transcript-1 is a ligand for the inhibitory human NKR-P1A receptor. *J. Immunol.* 175:7796–7799.

Schwab, S.R., J.P. Pereira, M. Matloubian, Y. Xu, Y. Huang, and J.G. Cyster. 2005. Lymphocyte sequestration through S1P lyase inhibition and disruption of S1P gradients. *Science*. 309:1735–1739. doi:10.1126/science.1113640

Shiow, L.R., D.B. Rosen, N. Brdicková, Y. Xu, J. An, L.L. Lanier, J.G. Cyster, and M. Matloubian. 2006. CD69 acts downstream of interferon-alpha/beta to inhibit S1P1 and lymphocyte egress from lymphoid organs. *Nature*. 440:540–544. doi:10.1038/nature04606

Shiow, L.R., D.W. Roadcap, K. Paris, S.R. Watson, I.L. Grigorova, T. Lebet, J. An, Y. Xu, C.N. Jenne, N. Föger, et al. 2008. The actin regulator coronin 1A is mutant in a thymic egress-deficient mouse strain and in a patient with severe combined immunodeficiency. *Nat. Immunol.* 9:1307–1315. doi:10.1038/ni.1662

Szabo, S.J., S.T. Kim, G.L. Costa, X. Zhang, C.G. Fathman, and L.H. Glimcher. 2000. A novel transcription factor, T-bet, directs Th1 lineage commitment. *Cell*. 100:655–669. doi:10.1016/S0092-8674(00)80702-3

Townsend, M.J., A.S. Weinmann, J.L. Matsuda, R. Salomon, P.J. Farnham, C.A. Biron, L. Gapin, and L.H. Glimcher. 2004. T-bet regulates the terminal maturation and homeostasis of NK and Valpha14i NKT cells. *Immunity*. 20:477–494. doi:10.1016/S1074-7613(04)00076-7

Vaessen, L.M., N.M. van Besouw, W.M. Mol, J.N. Ijzermans, and W. Weimar. 2006. FTY720 treatment of kidney transplant patients: a differential effect on B cells, naïve T cells, memory T cells and NK cells. *Transpl. Immunol.* 15:281–288. doi:10.1016/j.trim.2006.02.002

von Andrian, U.H., and T.R. Mempel. 2003. Homing and cellular traffic in lymph nodes. *Nat. Rev. Immunol.* 3:867–878. doi:10.1038/nri1222

Walzer, T., M. Bléry, J. Chaix, N. Fuseri, L. Chasson, S.H. Robbins, S. Jaeger, P. André, L. Gauthier, L. Daniel, et al. 2007a. Identification, activation, and selective in vivo ablation of mouse NK cells via NKp46. *Proc. Natl. Acad. Sci. USA*. 104:3384–3389. doi:10.1073/pnas.0609692104

Walzer, T., L. Chiossone, J. Chaix, A. Calver, C. Carozzo, L. Garrigue-Antar, Y. Jacques, M. Baratin, E. Tomasello, and E. Vivier. 2007b. Natural killer cell trafficking in vivo requires a dedicated sphingosine 1-phosphate receptor. *Nat. Immunol.* 8:1337–1344. doi:10.1038/ni1523

Watt, S.V., D.M. Andrews, K. Takeda, M.J. Smyth, and Y. Hayakawa. 2008. IFN-gamma-dependent recruitment of mature CD27(high) NK cells to lymph nodes primed by dendritic cells. *J. Immunol.* 181:5323–5330.

Xu, W., and J.J. Zhang. 2005. Stat1-dependent synergistic activation of T-bet for IgG2a production during early stage of B cell activation. *J. Immunol.* 175:7419–7424.

Published October 6, 2009

JEM

SUPPLEMENTAL MATERIAL

Jenne et al., http://www.jem.org/cgi/content/full/jem.20090525/DC1

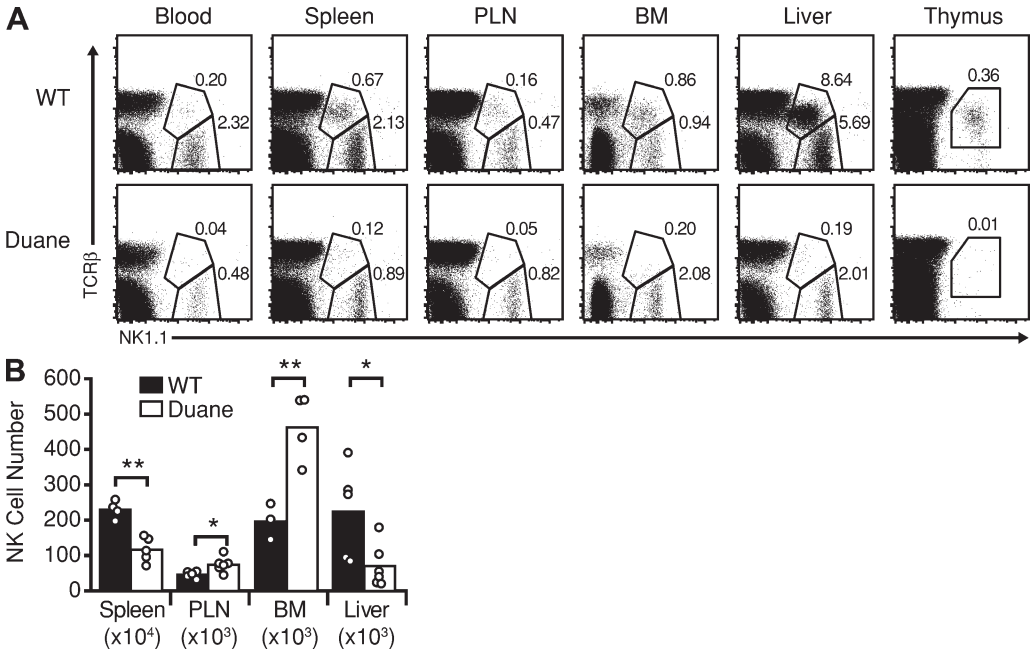

Figure S1. Identification of the ENU mutant Duane. (A) Representative flow cytometric analysis of various tissues from Duane and wild-type mice. Cells were gated on size. Numbers indicate the frequency of gated cells. Data are representative of at least two Duane and two wild-type mice in each of three independent experiments. (B) Absolute NK cell numbers in spleens, peripheral LNs (three nodes), BM (one femur and one tibia), and livers of Duane and wild-type mice. Data are derived from at least two independent experiments, each composed of at least two Duane and two wild-type mice. Bars represent mean values, and circles represent individual animals. PLN, peripheral LN. *, $P < 0.05$; **, $P < 0.001$.

Published October 6, 2009

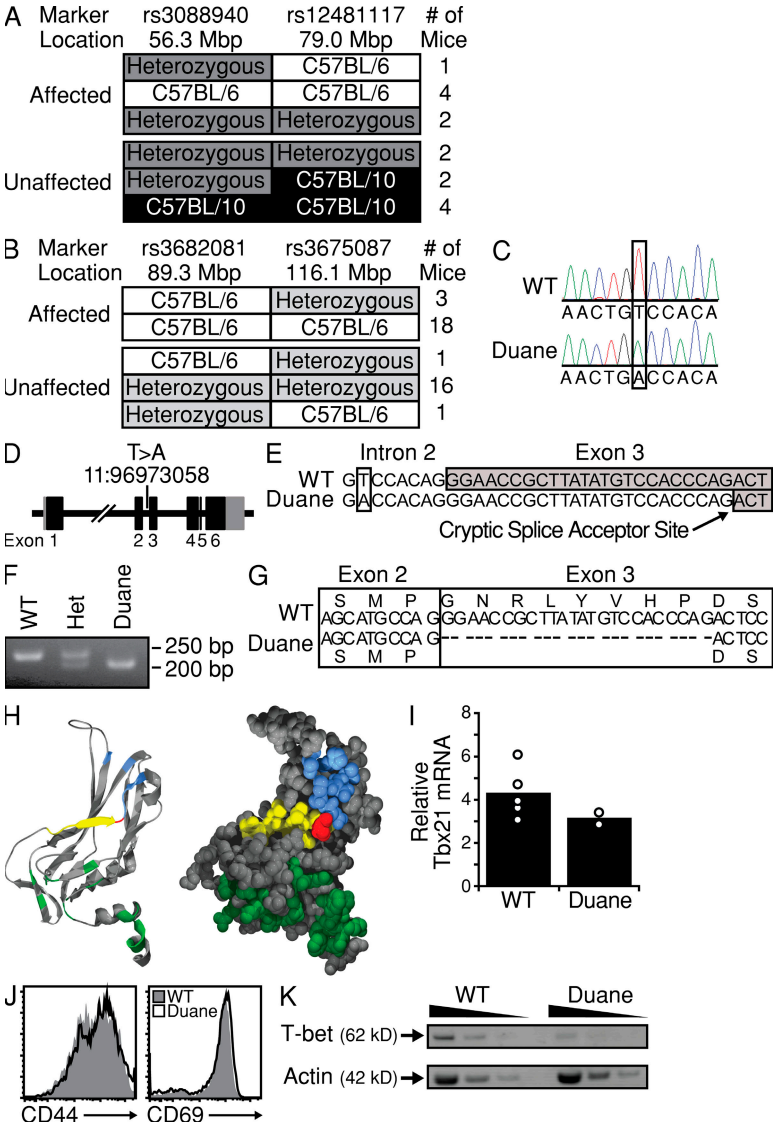

Figure S2. Mapping and Identification of a splice site mutation in Duane T-bet resulting in an eight–amino acid deletion and reduced T-bet protein expression. (A and B) The critical interval on chromosome 11 containing the causative mutation in Duane as defined by mapping SNPs that are polymorphic between Duane and either C57BL/10 (A) or CBA/J (B) mice. (C) Dideoxy sequencing chromatograph of genomic DNA from Duane and wild-type B6 mice revealing a T-to-A point mutation. (D) Schematic of the intron and exon organization of the *Tbx21* gene locus indicating the location of the Duane mutation. (E) Alignment of nucleotide sequences obtained from Duane and wild-type B6 genomic DNA. The Duane point mutation and the 5′ borders of exon 3 in each sequence are as indicated. (F) Amplification of T-bet transcripts from splenocyte cDNA generated from wild type, mice heterozygous for the Duane mutation (Het), and mice homozygous for the Duane mutation. Transcripts were amplified from at least two mice in two independent experiments. (G) Nucleotide alignment of cDNA sequences derived from Duane and wild-type B6 splenocytes. Boundaries of exon 2 and 3 are as indicated. Dashes indicate gaps corresponding to 24 nucleotides inserted into the Duane sequence to maximize alignment. Predicted amino acid sequences are included above and below the nucleotide alignment. (H) Predicted structure of the Duane T-bet protein derived from comparative protein analysis. Both ribbon and space filling models are displayed. Residues identified as responsible for DNA binding are colored green, those for protein dimerization are colored blue, and those predicted to be deleted by the Duane mutation are colored yellow. The single red residue corresponds to an amino acid known both to be important for dimerization and predicted to be deleted in Duane T-bet. (I) Quantitative PCR analysis of the expression of T-bet transcripts from wild-type and Duane splenic NK cells. Bars represent mean values, and circles represent individual PCR reactions. (J) Flow cytometric analysis of splenocytes cultured for 48 h under polyclonal T cell stimulation conditions (plate-bound anti-CD3 + anti-CD28). Populations were gated on $CD4^+$ $NK1.1^-$ cells. Data are representative of at least two individual animals in two independent experiments. (K) Western blot analysis of total cell lysates from the T cell splenocyte cultures in J. Samples were loaded in serial threefold dilutions. Data are representative of at least two individual animals in two independent experiments.

Published October 6, 2009

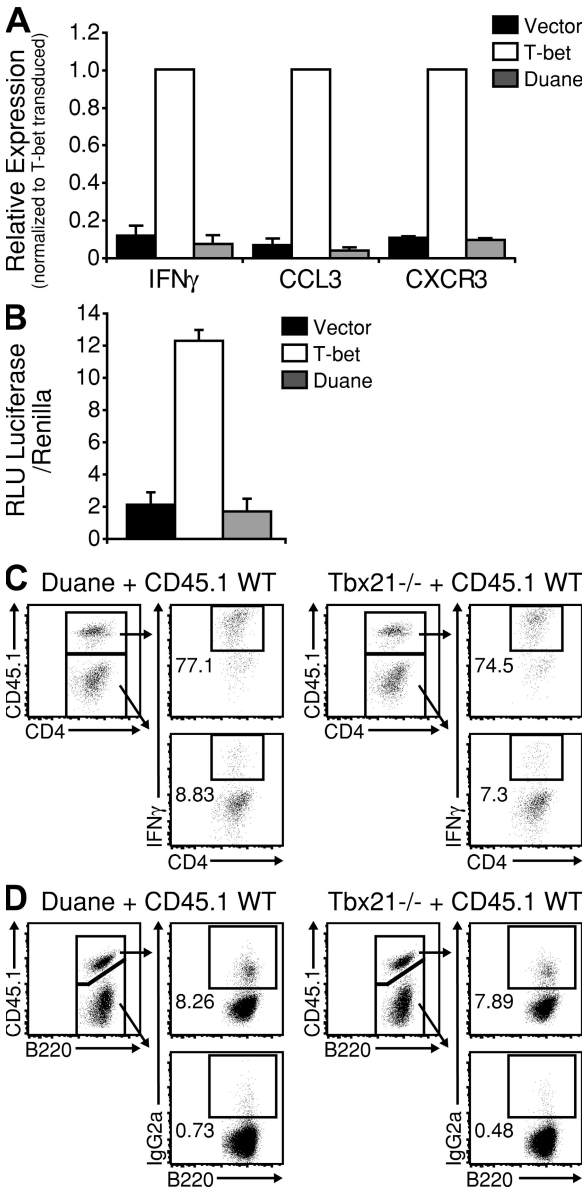

Figure S3. Duane T-bet appears to be functionally null. (A) The ENU mutation abolishes T-bet's ability to activate endogenous target genes. EL4 T lymphoma cells were transfected with constructs expressing either wild type T-bet (T-bet), the ENU mutant T-bet (Duane), or a pcDNA vector control (Vector). RNA was harvested from each transfection, and quantitative RT-PCR reactions were performed to monitor the endogenous gene expression of IFN-γ, CCL3, or CXCR3. All samples were first normalized to actin expression. Values are reported as the expression level for each target gene in the transfected sample relative to the level in the wild-type T-bet transduction. Bars represent means ± SD of two independent experiments. (B) The ENU mutation abolishes T-bet's ability to transactivate an IFN-γ promoter–reporter construct. EL4 T cells were transfected with an IFN-γ promoter–luciferase reporter construct, thymidine kinase–renilla control, and wild-type T-bet (T-bet), the ENU mutant T-bet (Duane), or a pcDNA vector control (Vector). Values are reported as relative luciferase light units (RLU) normalized to the control renilla expression for each transfected sample. Bars represent means ± SD of three independent experiments. (C) Duane or T-bet–deficient splenocytes were mixed with wild-type CD45.1 splenocytes and cultured for 5 d under Th1-inducing conditions (IL-2, IFN-γ, and anti–IL-12). Populations are gated on $CD4^+$ $NK1.1^-$ cells. Numbers indicate the frequency of gated cells. Data are representative of at least two independent experiments. (D) Duane or T-bet–deficient splenocytes were mixed with wild-type CD45.1 splenocytes and cultured for 4 d under conditions known to induce IgG2a Ig isotype switching (LPS, IFN-γ, and anti-IgM). Populations were gated $B220^+$ cells. Numbers indicate the frequency of gated cells. Data are representative of at lease two independent experiments.

Published October 6, 2009

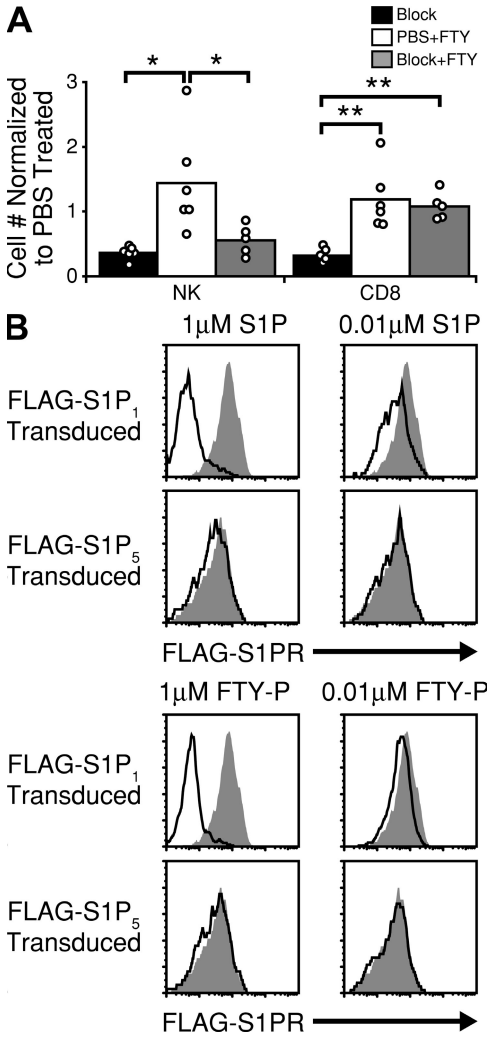

Figure S4. NK cell egress from LNs is FTY720 resistant. (A) Analysis of NK cell numbers in peripheral LNs from mice after 40 h of lymphocyte entry blockade. Mice were treated with integrin and L-selectin blocking antibody, 1 mg/kg FTY720, or a combination of blocking antibody and FTY720 for 40 h before analysis. Values are normalized to saline-treated controls. Bars represent mean values, and circles represent individual animals. Data are derived from more than three independent experiments. (B) Modulation of S1PR cell-surface expression. NFAT-GFP 2B4 hybridoma cells transduced with either FLAG-$S1P_1$ or FLAG-$S1P_5$ were left untreated (shaded) or incubated in the presence of the indicated concentrations of either S1P or FTY720-P (continuous line), and cell-surface expression of S1PR was detected by flow cytometry. Plots are representative of at least three experiments.

Published October 6, 2009

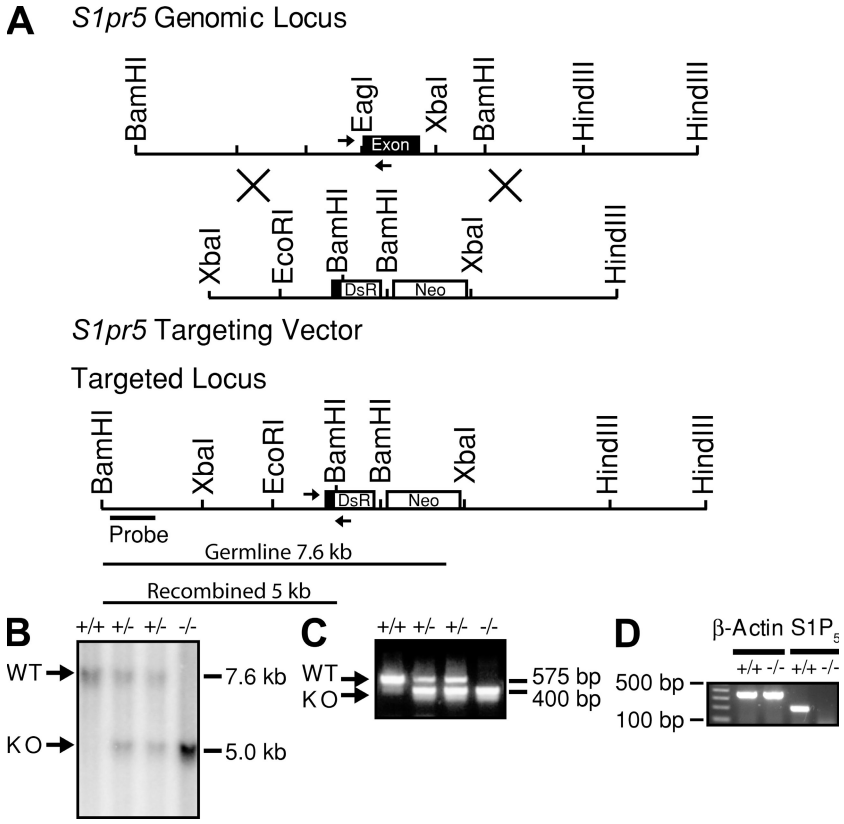

Figure S5. Generation of $S1P_5$–deficient mice. (A) Schematic diagram of the *S1pr5* genomic locus, targeting vector, and targeted allele. A portion of the $S1P_5$ coding region was removed, and Ds-Red (DsR) was inserted in frame into the deleted region. A neomycin resistance gene (Neo) under the control of the phosphoglycerate kinase promoter was also introduced into the targeting vector in an orientation reverse to that of the *S1pr5* genomic locus. Relevant restriction enzyme sites are shown. (B) BamHI-digested genomic DNA from one wild-type, two heterozygous, and one $S1P_5$-null mutant mice Southern blotted and probed with the indicated external probe. Resultant bands for wild-type alleles are 7.6 kb, whereas bands from recombined alleles are ∼5 kb. (C) PCR products from wild-type, heterozygous, and null mutant mice are shown. Primers used to amplify wild-type and mutant DNA elements are shown as arrows in the targeting schematic. Wild-type PCR products are ∼575 bp and products from mutant mice are ∼400 bp in length. Genotypes are indicated. (D) An absence of $S1P_5$ transcripts from the spinal cords of adult mice confirms the generation of null mutant mice. Spinal cord RNA from wild-type (+/+) and $S1P_5$-deficient (−/−) mice was reverse transcribed, and the presence of β-actin and $S1P_5$ transcripts was assayed for by PCR. PCR product sizes for β-actin and $S1P_5$ were ∼350 and 200 bp, respectively.

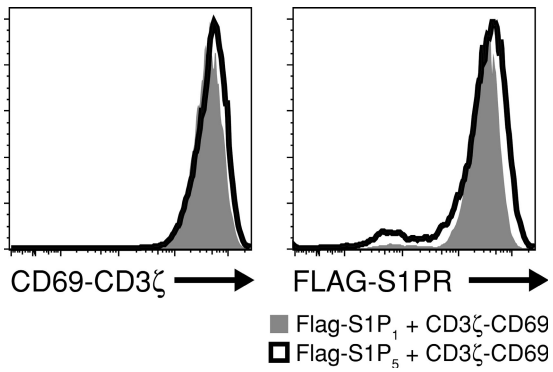

Figure S6. Cell-surface staining of transduced 2B4 hybridoma cells used for NFAT-GFP reporter assays. Representative flow cytometric analysis of transduced NFAT-GFP 2B4 cells stained for cell-surface expression of CD3ζ-CD69 and either FLAG-$S1P_1$ or FLAG-$S1P_5$. Data are representative of at least two independent experiments.

Published October 6, 2009

Table S1. PCR primer and probe sets used

Name	Type	Sequence (5′ to 3′)
Duane T-bet sequencing primers		
T-bet DNA exon 1	Sense	GGACCCAAGGAGCTTCATAA
	Antisense	GGCAGGGTAGCCATCAC
T-bet DNA exon 2	Sense	CTGGGGACGCCCTACTCT
	Antisense	AGCAACCTGCAGCTTCAAA
T-bet DNA exon 3	Sense	ACACAGGTGACTGCCACTGA
	Antisense	TCAGGAGCAGATGGAACAGA
T-bet DNA exon 4	Sense	AGAGATGAGGCCAGCTTGAG
	Antisense	GACCCCTGAAGCAGAGACAG
T-bet DNA exon 5	Sense	GAAGAGCAAGCAGCCAGTG
	Antisense	TAGTGGGCACCTTCCAATTC
T-bet DNA exon 6	Sense	TAAGGAAACCGAAGGCCAGT
	Antisense	GAAATACATCCAGACACCACTCTC
T-bet cDNA exon 2–4	Sense	GCAGTGTGGAAAGGCAGAAG
	Antisense	GGCTCTCCATCATTCACCTC
T-bet cDNA exon 1–5	Sense	CCAGCACCAGACAGAGATGA
	Antisense	TTGTCGATTTTCAGCTGAGTG
Quantitative PCR primers and probes		
β-Actin	Sense	TGGAATCCTGTGGCATCCATGAAAC
	Antisense	TAAAACGCAGCTCAGTAACAGTCCG
HPRT	Sense	AGGTTGCAAGCTTGCTGGT
	Antisense	TGAAGTACTCATTATAGTCAAGGGCA
	Probe	TGTTGGATACAGGCCAGACTTTGTTGGAT
$S1P_1$	Sense	GTGTAGACCCAGAGTCCTGCG
	Antisense	AGCTTTTCCTTGGCTGGAGAG
	Probe	CGGCTTGAGCGAGGCTGCTGTT
$S1P_2$	Sense	GGCCTAGCCAGTGCTCAGC
	Antisense	CCTTGGTGTAATTGTAGTGTTCCAGA
	Probe	CAGAGTACCTCAATCCTGA
$S1P_3$	Sense	GGAGCCCCTAGACGGGAGT
	Antisense	CCGACTGCGGGAAGAGTGT
	Probe	AGAACGAGAGCCTATTTT
$S1P_4$	Sense	CCTGGAACTCACTTTATAGACCAGG
	Antisense	AGAAAGCGTGCCATAGGCAG
	Probe	TGGCCTCGAACTCAGAAATCCGCC
$S1P_5$ (cell pellet)	Sense	GAGTGCCGGTTACAGGAGACTT
	Antisense	CGCTGCTGTGTCCTGCC
	Probe	CACAGTGCTCCAGTGGA
$S1P_5$ (spinal cord)	Sense	AGATTTCCAATAGCCGCTCTC
	Antisense	AGCTTGCCGGTGTAGTTGTAG
Tbx21	Sense	CGCTCAGCAACCACCTG
	Antisense	ATGGGAACATTCGCCGT
IFN-γ (WEHI-231)	Sense	AACATAAGCGTCATTGAATCA
	Antisense	GCTGGACCTGTGGGTTGT
IFN-γ (EL4)	Sense	CTACCTTCTTCAGCAACAGC
	Antisense	GCTCATTGAATGCTTGGCGC
CCL3	Sense	CATGACACTCTGCAACCAAG
	Antisense	GAGCAAAGGCTGCTGGTTTC
CXCR3	Sense	CAGCCAAGCCATGTACCTTG
	Antisense	CATAATCGTAGGGAGAGGTG
$S1P_5$ genotyping primers		
$S1P_5$N′ For	Sense	TCCTCGGTTCTAAACCTTCTC

Published October 6, 2009

Table S1. PCR primer and probe sets used *(Continued)*

Name	Type	Sequence (5′ to 3′)
DsRed Rev	Antisense	TTGGTCACCTTCAGCTTCACG
$S1P_5$KO Rev Gen	Antisense	CTCTAAAGCAATGGCCAAGAG